ABSTRACT

AN INVESTIGATION OF A FINITE
CAVITY IONIZATION THEORY

by

E. J. K. Cowdrey

A method of calculating the absorbed dose near an interface of two different materials undergoing X-ray irradiation has been developed by Charlton and Cormack (1962). Using a parallel-plate ionization chamber filled alternately with air, argon or hydrogen gas, Charlton (1967) tested the method using a 100 kvp X-ray spectrum and found fairly good agreement between theory and experiment. In the comparison, however, the full spectrum was represented by a simple three-component spectrum.

This thesis re-examines the method with a complete X-ray spectrum and a better ion chamber. The 56 kvcp spectrum used in the present study was determined by the techniques of gamma-ray scintillation spectroscopy. The chamber had large area plates, thus eliminating the necessity of correction for finite beam area, and acheived greater plate separations. Good agreement between theory and experiment was obtained over all plate separations for a filling gas of air.

AN INVESTIGATION OF A FINITE CAVITY IONIZATION THEORY

E. J. K. Cowdrey

A THESIS

in

Physics

Presented in Partial Fulfillment of the Requirements for the
Degree of Master of Science at
Sir George Williams University

March, 1970.

TABLE OF CONTENTS

ACKNOWLEDGEMENTS

The author expresses his gratitude to Dr. D. E. Charlton for suggesting the project and for his continued assistance throughout the course of research.

He also thanks Mr. J. Blaison and Mr. A. Christodoulopoulos, for technical help, and Mr. J. Lousteau, for constructing the ionization chamber.

ABSTRACT

A method of calculating the absorbed dose near an interface of two different materials undergoing X-ray irradiation has been developed by Charlton and Cormack (1962). Using a parallel-plate ionization chamber filled alternately with air, argon or hydrogen gas, Charlton (1967) tested the method using a 100 kvp X-ray spectrum and found fairly good agreement between theory and experiment. In the comparison, however, the full spectrum was represented by a simple three-component spectrum.

This thesis re-examines the method with a complete X-ray spectrum and a better ion chamber. The 56 kvcp spectrum used in the present study was determined by the techniques of gamma-ray scintillation spectroscopy. The chamber had large area plates, thus eliminating the necessity of correction for finite beam area, and acheived greater plate separations. Good agreement between theory and experiment was obtained over all plate separations for a filling gas of air.

CHAPTER I

RADIOLOGICAL QUANTITIES AND UNITS

1.1 General Terms

In recent years the International Commission on Radiological Units (ICRU) has set itself the task of putting radiological quantities and units on a concise basis. To understand the problem considered in this thesis it is necessary to be familiar with their definitions of certain terms.

To begin with,

> "Ionizing radiation is any radiation consisting of directly or indirectly ionizing particles or a mixture of both." (ICRU 1962)

In this definition,

> "Directly ionizing particles are charged particles (electrons, protons, α -particles, etc.) having sufficient kinetic energy to produce ionization by collision." (ICRU 1962)

Also,

> "Indirectly ionizing particles are uncharged particles (neutrons, photons, etc.) which can liberate directly ionizing particles or can initiate a nuclear transformation." (ICRU 1962)

In this study, the indirectly ionizing particles are X-ray photons and the directly ionizing particles are electrons liberated in the plates of an ionization chamber and in the gas (air) contained

between the plates.

It will be necessary to know the relative number of photons per square centimeter at each energy in the X-ray spectrum. These relative numbers are described by the particle fluence which the ICRU defines to be,

> "The <u>particle fluence</u> or <u>fluence</u> (Φ) of particles is the quotient of ΔN by Δa where ΔN is the number of particles which enter a sphere of cross-sectional area Δa ...."

$$\Phi = \frac{\Delta N}{\Delta a} . \quad \text{(ICRU 1962)}$$

When discussing photons it is customary to speak of the photon fluence rather than the particle fluence. The symbol, Δ , needs some explanation. Many of the quantities defined in this chapter have to be specified as functions of space or time and, in principle, they must therefore be determined for sufficiently small regions of space or intervals of time by some limiting procedure. The ICRU further explain that there are conceptual difficulties in taking such limits for quantities which depend upon the discrete interactions between radiations and atoms. The difficulties must be overcome by appropriate averaging procedures. The symbol Δ precedes the symbols for quantities that are involved in such averaging procedures.

It will be necessary to know also the energy fluence which is defined to be,

> "The <u>energy fluence</u> (F) of particles is the quotient of ΔE_F by Δa where ΔE_F is the sum of the energies, exclusive of rest energies, of all the particles which enter a sphere of cross-sectional area Δa ...."

$$F = \frac{\Delta E_F}{\Delta a} . \quad \text{(ICRU 1962)}$$

In Chapter II the expression "linear energy transfer", symbolized by L or LET, will be used. The ICRU define L as,

> "The linear energy transfer (L) of charged particles in a medium is the quotient of dE_L by dl where dE_L is the average energy locally imparted to the medium by a charged particle of specified energy in traversing a distance dl."

$$L = \frac{dE_L}{dl}. \quad \text{(ICRU 1962)}$$

The term "locally imparted" may refer either to a maximum distance from the track or to a maximum value of discrete energy loss by the particle beyond which losses are no longer considered local.

A term related to L is the mass stopping power, defined to be,

> "The mass stopping power (S/ρ) of a material for charged particles is the quotient of dE_s by the product of dl and ρ, where dE_s is the average energy lost by a charged particle of specified energy in traversing a path length dl, and ρ is the density of the medium."

$$\frac{S}{\rho} = \frac{1}{\rho}\frac{dE_s}{dl}. \quad \text{(ICRU 1962)}$$

dE_s denotes energy lost due to ionization, electronic excitation and radiation. For some purposes it is desirable to consider stopping power with the exclusion of bremsstrahlung losses. In this case $\frac{S}{\rho}$ is multiplied by an appropriate factor that is less than unity.

It is important to realize that the concept of linear energy transfer is different from that of stopping power. The former refers to energy imparted within a limited volume, the latter to loss of energy regardless of where this energy is absorbed.

Berger and Seltzer (1964) have prepared extensive tables of mass stopping power as a function of electron energy for many materials. To calculate the mass stopping power due to collision, they utilize

a formula derived from Bethe's stopping-power theory:

$$-\frac{1}{\rho}\left(\frac{dE}{dx}\right)^{-}_{col} = \frac{2\pi N_a r_o^2 mc^2}{\beta^2}\,\frac{Z}{A}\left\{\ln\left[\frac{\tau^2(\tau+2)}{2(I/mc^2)^2}\right] + F^{-}(\tau) - \delta\right\}$$

where

$F^{-}(\tau) = 1 - \beta^2 + \left[\tau^2/8 - (2\tau+1)\ln 2\right]/(\tau+1)^2$, for electrons

mc^2 = rest energy = 0.510976 Mev

τ = kinetic energy in units of mc^2

$\beta = \left[\tau(\tau+2)\right]^{1/2}/(\tau+1)$ = velocity/c

Z = atomic number

A = atomic weight

ρ = density

I = mean excitation energy

δ = density effect correction

N_a = Avogadro's number = 6.02486×10^{23} electron/mole

$r_o^2 = (e^2/mc^2)^2 = 7.94030 \times 10^{-26}$ cm^2.

Berger and Seltzer define the range, $r^{-}(\tau)$, of an electron as,

$$r^{-}(\tau) = \int_0^{\tau}\left[-\frac{1}{\rho}\left(\frac{dE}{dx}\right)^{-}_{tot}\right]^{-1} d\tau',$$

where

$$-\frac{1}{\rho}\left(\frac{dE}{dx}\right)^{-}_{tot} = -\frac{1}{\rho}\left(\frac{dE}{dx}\right)^{-}_{col} - \frac{1}{\rho}\left(\frac{dE}{dx}\right)^{-}_{rad}.$$

$-\frac{1}{\rho}\left(\frac{dE}{dx}\right)^{-}_{rad}$ is the mass stopping power due to energy loss by bremsstrahlung. $r^{-}(\tau)$ is called the continuous-slowing-down-approximation (c.s.d.a.) range and will be necessary in calculations to be performed in this study.

One more term, the mass attenuation coefficient, will be defined in this section. The definition given by the ICRU is,

> "The mass attenuation coefficient (μ/ρ) of a material for indirectly ionizing particles is the quotient of dN by the product of ρ, N, and dl, where N is the number of particles incident normally upon a layer of thickness dl and density ρ, and dN is the number of particles that experience interactions in this layer."

$$\frac{\mu}{\rho} = \frac{1}{\rho N}\frac{dN}{dl}. \quad \text{(ICRU 1962)}$$

The term "interactions" refers to processes whereby the energy or direction of the indirectly ionizing particles is altered. For photons, these processes include the photoelectric effect, the Compton effect, pair-production and coherent scattering. For X or gamma radiation, therefore,

$$\frac{\mu}{\rho} = \frac{\tau}{\rho} + \frac{\sigma}{\rho} + \frac{\sigma_{coh}}{\rho} + \frac{\kappa}{\rho}$$

where $\frac{\tau}{\rho}$ is the mass photoelectric attenuation coefficient, $\frac{\sigma}{\rho}$ is the total Compton mass attenuation coefficient, $\frac{\sigma_{coh}}{\rho}$ is the mass attenuation coefficient for coherent scattering and $\frac{\kappa}{\rho}$ is the pair-production mass attenuation coefficient.

1.2 Energy Absorption in Media exposed to Ionizing Radiation

Reference has already been made to the term "energy imparted" without stating the exact meaning. The ICRU define this term to be,

> "The <u>energy imparted</u> by ionizing radiation to the matter in a volume is the difference between the sum of the energies of all the directly and indirectly ionizing particles which have entered the volume and the sum of the energies of all those which have left it, minus the energy equivalent of any increase in rest mass that took place in nuclear or elementary

particle reactions within the volume." (ICRU 1962)

The quantity, absorbed dose, is now defined as,

> "The absorbed dose (D) is the quotient of ΔE_D by Δm, where ΔE_D is the energy imparted by ionizing radiation to the matter in a volume element, Δm is the mass of the matter in that volume element ...."

$$D = \frac{\Delta E_D}{\Delta m}. \quad \text{(ICRU 1962)}$$

The special unit of absorbed dose is the rad.

$$1 \text{ rad} = 100 \text{ ergs/g}.$$

One may now introduce the concept of the kerma, short for kinetic energy released in material. The ICRU define the kerma to be,

> "The kerma (K) is the quotient of ΔE_K by Δm, where ΔE_K is the sum of the initial kinetic energies of all the charged particles liberated by indirectly ionizing particles in a volume element of the specified material, Δm is the mass of the matter in that volume element ...."

$$K = \frac{\Delta E_K}{\Delta m}. \quad \text{(ICRU 1962)}$$

Since ΔE_K is the sum of the initial kinetic energies of the charged particles liberated by the indirectly ionizing particles, it includes not only the kinetic energy these charged particles expend in collisions but also the energy they radiate in bremsstrahlung. The energy of any charged particle is also included when these are produced in secondary processes occurring within the volume element. Thus, the energy of Auger electrons is part of ΔE_K.

The kerma is a useful quantity when electronic equilibrium exists for then the kerma is equal to the absorbed dose, a result which

will be demonstrated by calculation in Chapter II. Electronic equilibrium is said to exist at a point in a medium when that point is surrounded by a sphere of the medium of radius at least equal to the range of the maximum energy electrons liberated in the medium.

The kerma can be calculated by means of the mass energy transfer coefficient which is defined as,

> "The <u>mass energy transfer coefficient</u> (μ_K/ρ) of a material for directly ionizing particles is the quotient of dE_K by the product of E, ρ, and dl, where E is the sum of the energies (excluding rest energies) of the indirectly ionizing particles incident normally upon a layer of thickness dl and density ρ, and dE_K is the sum of the kinetic energies of all the charged particles liberated in this layer."

$$\frac{\mu_K}{\rho} = \frac{1}{E\rho}\frac{dE_K}{dl}. \quad \text{(ICRU 1962)}$$

The relation between energy fluence and kerma may now be written,

$$K = F\frac{\mu_K}{\rho}.$$

The ICRU goes on to say that $\frac{\mu_K}{\rho}$ can be written as the sum of coefficients corresponding to the photoelectric effect, the Compton effect and pair-production. The clearest formulation, however, is given by Berger (1961). One may write,

$$\frac{\mu_K}{\rho} = \frac{\tau}{\rho}F_\tau + \frac{\sigma}{\rho}f_c + \frac{\kappa}{\rho}f_\kappa,$$

where F_τ, f_c and f_κ are conversion factors which indicate, for the respective interactions, the fraction of the photon energy which is eventually converted into kinetic energy of electrons and is dissipated to the medium via collision losses as ionization and excitation. The factors $\frac{\tau}{\rho}$, $\frac{\sigma}{\rho}$ and $\frac{\kappa}{\rho}$ are defined in the discussion of

$\frac{\mu}{\rho}$ (section 1.1).

τ may be written as a sum of coefficients corresponding to the K, L, M, ... shells of an atom:

$$\tau = \tau^K + \tau^L + \tau^M + \ldots.$$

F_τ is then defined by,

$$\tau F_\tau = \tau^K F_\tau^K + \tau^L F_\tau^L + \tau^M F_\tau^M + \ldots,$$

where F_τ^K, F_τ^L, F_τ^M, etc., are conversion factors for different shells. If the n^{th} shell with binding energy ϕ_n absorbs a photon of energy $h\nu$, Berger gives,

$$F_\tau^n(h\nu) = \frac{1}{h\nu}(h\nu - \phi_n) + \frac{\phi_n}{h\nu}\left[1 - \frac{F_n\bar{E}_n}{\phi_n}\right]$$

where the first term refers to photoelectrons and the second to Auger electrons. F_n is the mean fluorescence yield and $\bar{E}_n$ is the mean energy of the fluorescence photons. Writing

$$f_\tau^n = 1 - \frac{\phi_n}{h\nu}$$

$$f_\tau^{Auger} = \frac{\phi_n - \delta}{h\nu}$$

where $\delta = F_n\bar{E}_n$, the partial kermas, $\Delta K(E_o)$, may be defined as,

$$\left[\Delta K(E_o)\right]_\tau^n = \Delta F(h\nu) \cdot \frac{\tau^n}{\rho} \cdot f_\tau^n$$

for the photoelectric effect in the n^{th} shell (E_o = energy of the photoelectrons = $h\nu - \phi_n$) and

$$\left[\Delta K(\bar{E}_o)\right]_{Auger} = \Delta F(h\nu) \cdot \frac{\tau^n}{\rho} \cdot f^{Auger}_{\tau}$$

for the Auger effect associated with the n^{th} shell ($\bar{E}_o$ is now the average energy of the Auger electrons). $\Delta F(h\nu)$ is the energy fluence of photons of energy $h\nu$ and is related to the energy fluence previously defined by,

$$F = \sum_{h\nu} \Delta F(h\nu).$$

Similarly, a partial kerma can be defined for the Compton effect. $\sigma \cdot f_c$ is just the true Compton absorption coefficient, σ_a, defined by Evans (1958). Therefore,

$$\left[\Delta K(\bar{E}_o)\right]_{Compton} = \Delta F(h\nu) \cdot \frac{\sigma}{\rho} \cdot f_c.$$

To simplify calculations the Compton spectrum is assigned an average energy of $\bar{E}_o = \frac{\sigma_a}{\sigma} \cdot h\nu$ where σ is the Compton component of the linear attenuation coefficient, μ. This is a good enough approximation since the Compton electrons play a relatively minor role in the problem to be discussed in this thesis.

Pair-production is not discussed further since it does not occur at the energies of interest in this study.

An important quantity is the exposure, which is defined to be,

> "The <u>exposure</u> (X) is the quotient of ΔQ by Δm, where ΔQ is the sum of the electrical charges on all ions of one sign produced in air when all the electrons (negatons and positrons), liberated by photons in a volume element of air whose mass is Δm, are completely stopped in air ...."
>
> $$X = \frac{\Delta Q}{\Delta m}.$$ (ICRU 1962)

The special unit of exposure is the roentgen (R).

$$1R = 2.58 \times 10^{-4} \text{ coulombs/kg.}$$

The next term defined in this section is:

> "The average energy (W) expended in a gas per ion pair formed is the quotient of E by N_w, where N_w is the average number of ion pairs formed when a charged particle of initial energy E is completely stopped in the gas."

$$W = \frac{E}{N_w}. \quad \text{(ICRU 1962)}$$

The ions arising from the absorption of bremsstrahlung emitted by the charged particles are not to be counted in N_w. For air,

$$W(\text{air}) = 33.7 \pm 0.15 \text{ ev/ion pair.} \quad \text{(ICRU 1962)}$$

It is interesting to calculate the energy absorption in air due to an exposure of 1R. This is just,

$$2.58 \times 10^{-4} \text{ (coul/kg)} \times \frac{1}{1.602 \times 10^{-19}} \text{ (pairs/coul)} \times 33.7 \text{ (ev/ion paiir)}$$
$$\times 1.602 \times 10^{-12} \text{ (ergs/ev)} \times 10^{-3} \text{ (kg/g)}$$
$$= 86.9 \text{ ergs/g.}$$

Knowledge of the exposure is essential when discussing the absorbed dose. Suppose, for example, that one is irradiating a sample of matter with X-rays. Clearly, any value of absorbed dose can be obtained simply by using a sufficiently long irradiation time. Accordingly, one speaks not of the number of rads but rather of the number of rads per roentgen, and the absorbed dose is completely specified. The way in which an X-ray spectrum is normalized to 1R

is given in section 1.3.

The last topic which will be discussed in this section is the Bragg-Gray theory developed by Bragg (1912) and Gray (1929). Gray suggested that the absorbed dose, D_m, in a medium may be related to the absorbed dose, D_g, in a gas-filled cavity within the medium by,

$$\frac{D_m}{D_g} = \frac{(S/\rho)_m}{(S/\rho)_g},$$

where $(S/\rho)_m$ and $(S/\rho)_g$ are the mass stopping powers of the medium and gas respectively. The absorbed dose in the gas may be determined by collecting the ions formed in it and is given by,

$$D_g = J_g W,$$

where J_g is the number of ion pairs formed per unit mass of gas and W is the average energy required to produce an ion pair. Therefore,

$$D_m = J_g W \frac{(S/\rho)_m}{(S/\rho)_g}.$$

The conditions for the validity of the theory are briefly summarized as:

1. The cavity must have dimensions such that only a small fraction of a particle's energy is dissipated in it, i.e., the range of most of the particles entering the cavity must be much greater than the cavity dimensions.
2. The ionization of the gas by electrons generated in the gas should be small compared to the total ionization.
3. The cavity should be small enough so that the electron flux through the cavity is characteristic of the material

surrounding the cavity.

4. The energy dissipation within the medium should be uniform over the volume of the medium surrounding the cavity.

It will be shown in Chapter II that the absorbed dose in the gas contained within an ionization chamber approaches the Bragg-Gray limit as the plate separation tends to zero.

1.3 Terms describing an X-ray Spectrum

If $\Delta\Phi(h\nu)\cdot d(h\nu)$ is the fluence (photons/cm^2) of photons with energies between $h\nu$ and $h\nu+d(h\nu)$ of a continuous X-ray spectrum, then the average energy, $\overline{h\nu}$, of the spectrum is just,

$$\overline{h\nu} = \frac{\int_0^{h\nu_{max}} \Delta\Phi(h\nu)\cdot h\nu\cdot d(h\nu).}{\int_0^{h\nu_{max}} \Delta\Phi(h\nu)\cdot d(h\nu)}$$

Usually, an analytical expression for $\Delta\Phi(h\nu)$ is not known and the integrals must be replaced by sums:

$$\overline{h\nu} = \frac{\sum_{h\nu} \Delta\Phi(h\nu)\cdot h\nu\cdot\Delta(h\nu).}{\sum_{h\nu} \Delta\Phi(h\nu)\cdot\Delta(h\nu)}$$

Often, it is necessary to normalize a spectrum to some exposure. If, for example, a spectrum is said to be normalized to one roentgen, then the $\Delta\Phi(h\nu)$ satisfy,

$$\sum_{h\nu} \Delta\Phi(h\nu)\cdot h\nu\cdot\frac{\mu_K^{air}}{\rho}\cdot\Delta(h\nu) = 86.9 \text{ ergs/g},$$

where $\frac{\mu_K^{air}}{\rho}$ is the mass energy transfer coefficient for air for photons of energy $h\nu$. Evidently, if one has only relative photon fluence, $\Delta\Phi(h\nu)\cdot\Delta(h\nu)$, and wants to normalize the spectrum to one roentgen

then each $\Delta\Phi(h\nu)$ must be multiplied by a factor, N, where,

$$N = \frac{86.9}{\sum_{h\nu} \Delta\Phi(h\nu)\cdot h\nu \cdot \frac{\mu_K^{air}}{\rho}\cdot \Delta(h\nu)}.$$

Next to be discussed is the half-value-thickness (H.V.T.) of a spectrum. Suppose a thickness $t_{\frac{1}{2}}$ of material is placed in an X-ray beam. This thickness is the H.V.T. if it satisfies,

$$T_{\frac{1}{2}} = \frac{\sum_{h\nu} \Delta\Phi(h\nu)\cdot h\nu \cdot \frac{\mu_K^{air}}{\rho} \exp\left[-\mu \cdot t_{\frac{1}{2}}\right]\cdot \Delta(h\nu)}{\sum_{h\nu} \Delta\Phi(h\nu)\cdot h\nu \cdot \frac{\mu_K^{air}}{\rho}\cdot \Delta(h\nu)} = 0.5$$

where μ is the linear attenuation coefficient for the material for photons of energy $h\nu$ and T is a dimensionless quantity called the transmission. By choosing different values of t a graph of T versus t, known as the exposure transmission curve for the X-ray spectrum, can be calculated. Since dosemeters (such as the Victoreen condenser r-meter) may be used to obtain the curve experimentally, an important check can be made on the accuracy with which one has determined a spectrum. The results of this check on the 56 kvcp spectrum used in the present study will be given in Chapter III where the calculated and measured H.V.T.'s are compared.

Clearly, monoenergetic photons of energy $h\nu_{eff}$, where $h\nu_{eff}$ has a corresponding linear attenuation coefficient given by,

$$\mu_{eff} = \frac{0.693}{t_{\frac{1}{2}}},$$

have the same H.V.T. as the spectrum. $h\nu_{eff}$, known as the effective photon energy, is often given as a specification of an X-ray spectrum.

CHAPTER II

THEORETICAL CALCULATION OF ABSORBED DOSE IN A PARALLEL-PLATE IONIZATION CHAMBER

2.1 Absorbed Dose under Conditions of Electronic Equilibrium

Suppose that a point P in a medium is surrounded by a sphere of that material of radius equal to the range of the maximum energy electrons liberated in the medium by photons (fig. 2.1). If N_o electrons are generated isotropically per cubic centimeter, each with an initial energy, E_o, and a corresponding range, R_o, then the equilibrium value for the energy dissipated by the electrons per cubic centimeter at P is given by

$$\Delta \mathcal{D}(E_o) = \int_0^{2\pi} \left\{ \int_0^{\pi} \left[\int_0^{R_o} \frac{N_o\, r^2 \sin\theta}{4\pi r^2} \left(\frac{dE}{dR}\right)_P dr \right] d\theta \right\} d\phi \qquad 2.1$$

where $\left(\frac{dE}{dR}\right)_P$ is the LET of the electrons as they pass P, and the other parameters are as shown in fig. 2.1. This expression, as well as all others derived in this chapter, were originally derived by Charlton and Cormack (1962).

It is assumed that all energy loss by electrons is dissipated in the medium; i.e., there is no energy escape of bremsstrahlung, etc. It is therefore applicable to electron energies up to a few hundred kev in materials of low atomic number. For electron energies between 20 and 200 kev, the relation between range and energy can be expressed by the empirical relationship

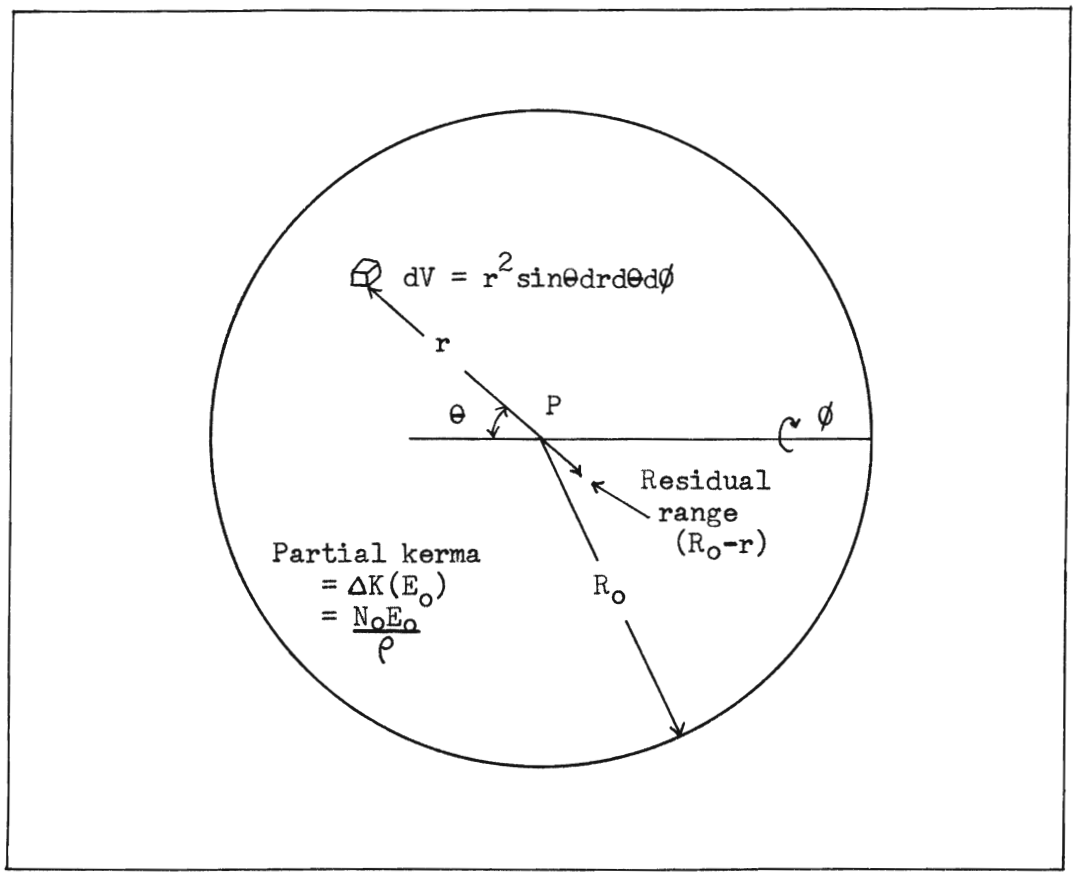

Figure 2.1 The equilibrium sphere.

$$R = AE^m \qquad 2.2$$

where R is the range (assumed to be in a straight line) travelled by an electron as its energy drops from E to zero, and A and m are constants which may be determined from experimental data. The LET is given by

$$\frac{dE}{dR} = \frac{1}{m}\left(\frac{1}{A}\right)^{\frac{1}{m}} R^{\left(\frac{1}{m}\right)-1} \qquad 2.3$$

and may be expressed in terms of the residual range (R_o-r). Substitution of this expression into equation 2.1 gives

$$\Delta \mathcal{D}(E_o) = \frac{N_o}{4\pi}\int_0^{2\pi}\left\{\int_0^{\pi}\sin\theta\left[\int_0^{R_c}\frac{1}{m}\left(\frac{1}{A}\right)^{\frac{1}{m}}(R_o-r)^{\left(\frac{1}{m}\right)-1}dr\right]d\theta\right\}d\phi$$

$$= \frac{N_o}{4\pi}\int_0^{2\pi}\left[\int_0^{\pi}\left(\frac{1}{A}\right)^{\frac{1}{m}} R_o^{\frac{1}{m}}\sin\theta\, d\theta\right]d\phi$$

$$= \frac{N_oE_o}{4\pi}\int_0^{2\pi}\left(\int_0^{\pi}\sin\theta\, d\theta\right)d\phi$$

$$\Delta \mathcal{D}(E_o) = N_oE_o \qquad 2.4$$

The absorbed dose at P is given by $\Delta D(E_o) = \frac{\Delta \mathcal{D}(E_o)}{\rho}$ where ρ is the density of the medium. Furthermore, since $\frac{N_oE_o}{\rho} = \Delta K(E_o)$, where $\Delta K(E_o)$ is the partial kerma, then $\Delta D(E_o) = \Delta K(E_o)$. That is, the absorbed dose in a medium under electronic equilibrium equals the (partial) kerma.

Equation 2.4 is a statement of electronic equilibrium and is valid under the following conditions:

1. If a point is surrounded by a sphere of medium (or a greater volume) of radius equal to the maximum range of electrons

generated by photons passing through the medium, then the energy dissipated at the point is equal to the energy generated by photons in the form of electron kinetic energy.

2. It is assumed that the number of electrons generated per unit volume is constant throughout the sphere.

3. In this treatment the continuous-energy-loss model has been used; i.e., the electrons are assumed to lose energy continuously along their paths, and the effects of δ rays are neglected.

2.2 Description of the Dose Distribution inside an Ion Chamber

The dose distribution between the plates of an ionization chamber undergoing X-ray irradiation is best shown by a diagram (fig. 2.2).

The horizontal straight portion of the dose distribution curve represents the absorbed dose at points in the gas at distances from the plates greater than the range of the maximum energy electrons liberated in the plates. The absorbed dose at these points is due to electrons liberated in the gas and, as shown in section 2.1, equals the kerma. At points closer to the plates, the curve shows a rise since electrons liberated in the plates can reach these points in the gas and increase the dose. The effect is uncompensated by electrons from the gas travelling into the plates since more electrons travel from the plates into the gas than from the gas into the plates.

The distribution is symmetrical about the center of the chamber, a consequence of assuming that the X-ray spectrum is uniform throughout the gas and just within the inside surfaces of the plates. That is, attenuation by the gas is considered insignificant. It is

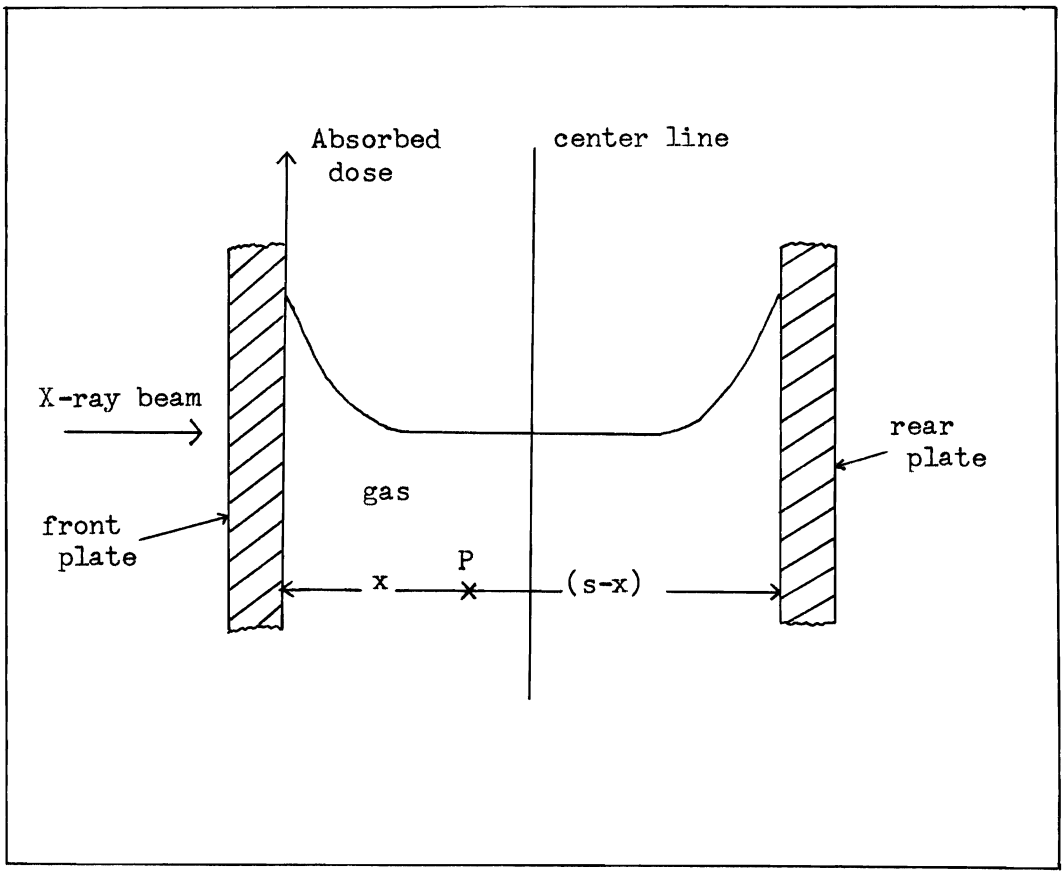

Figure 2.2 Dose distribution inside an ionization chamber. It is assumed that the atomic number of the wall material is greater than that of the gas.

also assumed that the electrons are liberated isotropically by the photons.

The theoretical distribution may be averaged and compared with an experimental measurement determined from the ionization current.

2.3 The Contribution of the Walls to the Absorbed Dose in a Gas contained within an Ionization Chamber

To calculate the absorbed dose in the gas of density ρ due to the walls of density ρ', consider first the contribution of only one wall as depicted in fig. 2.3. The dotted line indicates the boundary of the equilibrium sphere of radius R_o. The solid curved line represents a "cap" to this equilibrium sphere. Only electrons from the wall liberated within the cap can reach point P.

Let N_o' be the number of electrons of energy E_o' liberated per unit volume in the wall. The partial kerma will be denoted by $\Delta K'(E_o')$. The range of electrons of energy E_o' in the wall material will be called R_o' to distinguish it from the range, R_o, of the same energy electrons in the gas. The ratio of R_o to R_o' will be called the linear range ratio, n.

The range-energy relation in the wall material is assumed to be

$$R_w(E) = \frac{AE^m}{n}. \qquad 2.5$$

The limits for the integration with respect to r become

$$r_{min} = \frac{x}{\cos\theta} \qquad r_{max} = \frac{x}{\cos\theta} + \frac{R_o - (x/\cos\theta)}{n}.$$

The energy dissipated at P per unit volume by electrons generated in the wall then becomes

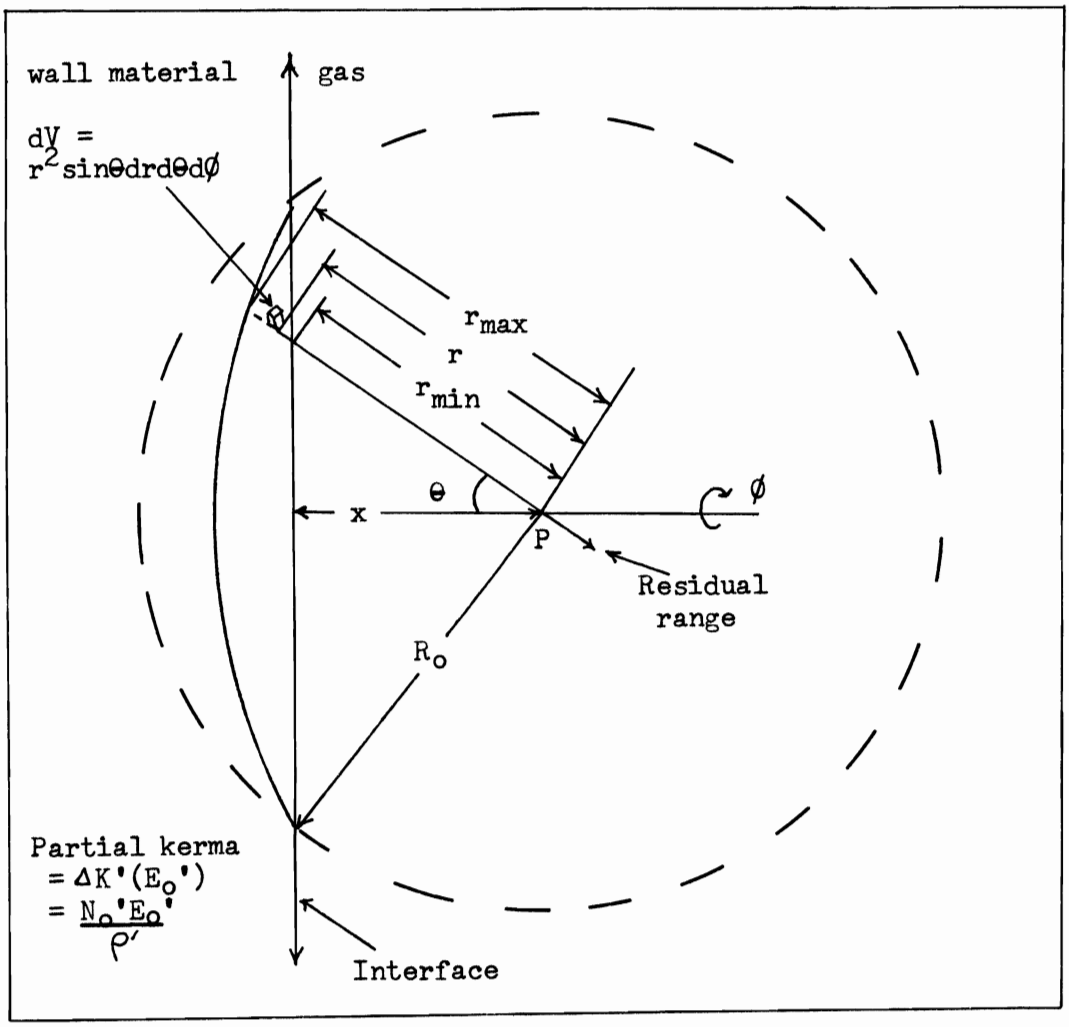

Figure 2.3 A diagram illustrating the geometry used to calculate the absorbed dose due to one wall at a point P in the gas.

$$\Delta \mathcal{D}_w(x,E_o') = \frac{N_o'}{4\pi}\int_0^{\arccos(x/R_o)} \sin\theta \cdot \left(\int_0^{2\pi}\left\{\int_{r_{min}}^{r_{max}} \frac{1}{m}\left(\frac{1}{A}\right)^{\frac{1}{m}}\left[R_o - n\left(r - \frac{x}{\cos\theta}\right) - \frac{x}{\cos\theta}\right]^{\left(\frac{1}{m}\right)-1} dr\right\}d\phi\right)d\theta$$

where $\left[n\left(r - \frac{x}{\cos\theta}\right) + \frac{x}{\cos\theta}\right]$ is the equivalent gas path of electrons that travel a distance r part of which is in the wall material. This equation reduces to

$$\Delta \mathcal{D}_w(x,E_o') = \frac{N_o'E_o'}{2n}\int_0^{\arccos(x/R_o)} \left(1 - \frac{x}{R_o\cos\theta}\right)^{\frac{1}{m}} \sin\theta\, d\theta$$

$$\text{or } \Delta \mathcal{D}_w(x,E_o') = \frac{N_o'E_o'}{n} P(x,R_o) \qquad 2.6$$

where the geometrical factor

$$P(x,R_o) = \frac{1}{2}\int_0^{\arccos(x/R_o)} \left(1 - \frac{x}{R_o\cos\theta}\right)^{\frac{1}{m}} \sin\theta\, d\theta. \qquad 2.7$$

The absorbed dose at P due to the wall is $\Delta D_w(x,E_o') = \frac{\Delta \mathcal{D}_w(x,E_o')}{\rho}$.

Since $\frac{N_o'E_o'}{\rho'} = \Delta K'(E_o')$, then

$$\Delta D_w(x,E_o') = \frac{\Delta \mathcal{D}_w(x,E_o')}{\rho}$$

$$= \frac{\Delta K'(E_o')}{n}\cdot\frac{\rho'}{\rho}\cdot P(x,R_o)$$

$$\Delta D_w(x,E_o') = \frac{\Delta K'(E_o')}{n_m}\cdot P(x,R_o) \qquad 2.8$$

where n_m is the mass range ratio, $\frac{R_o\rho}{R_o'\rho'}$. $P(x,R_o)$ has been extensively evaluated by Howarth (1965) and is shown in fig. 2.4. It is important to note that the ranges R_o and R_o' are taken to be 0.7 times the c.s.d.a. ranges. In this way, the reduction due to scattering of the effective distance travelled by the electrons is

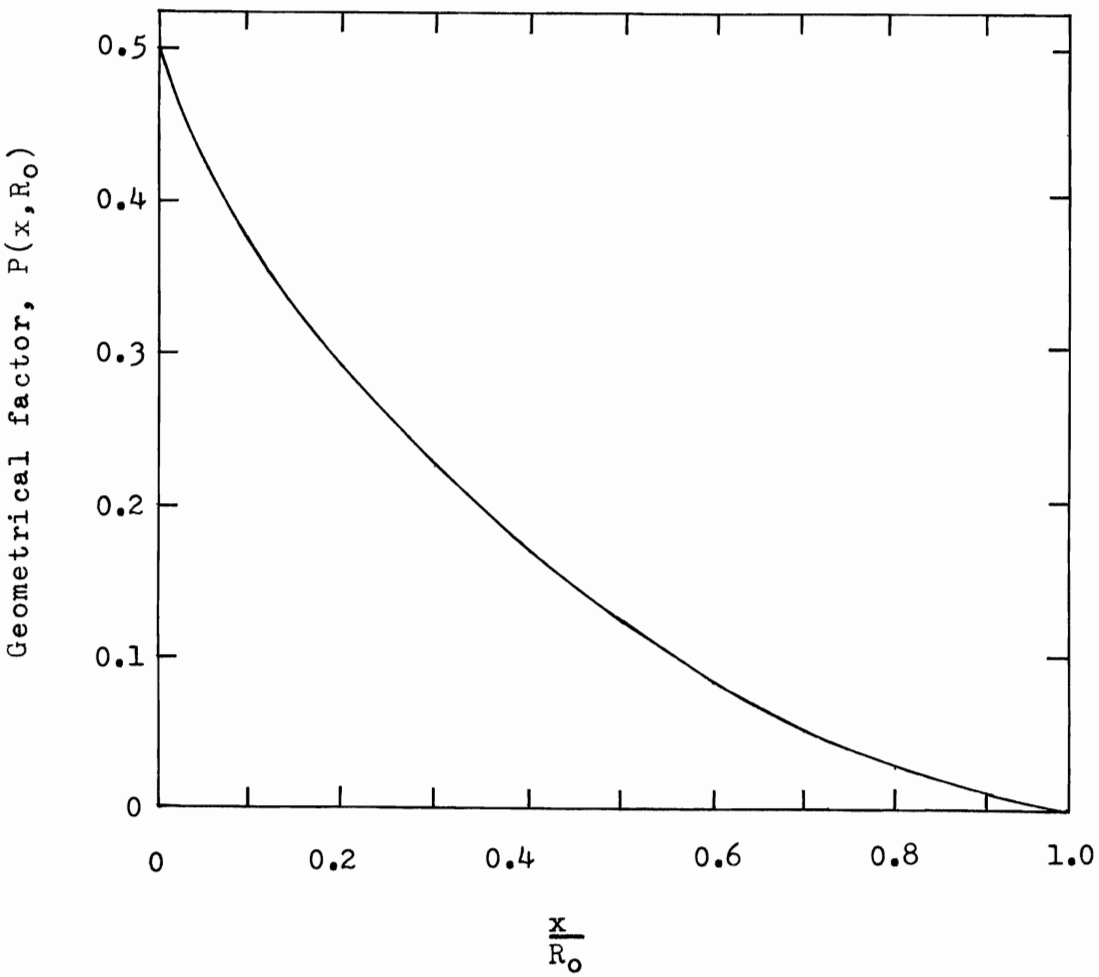

Figure 2.4 Geometrical factor for a plane interface.

taken into account.

Clearly, if two walls are present as indicated in fig. 2.2, the dose at P due to the walls is just

$$\Delta D_{ww}(x,E_o) = \frac{\Delta K'(E_o')}{n_m}\cdot P(x,R_o) + \frac{\Delta K'(E_o')}{n_m}\cdot P(s-x,R_o). \qquad 2.9$$

Furthermore, if there is a spectrum of energies, E_o', the wall contribution becomes

$$\Delta D_{ww}(x) = \sum_{E_o'} \frac{\Delta K'(E_o')}{n_m}\cdot P(x,R_o) + \sum_{E_o'} \frac{\Delta K'(E_o')}{n_m}\cdot P(s-x,R_o). \qquad 2.10$$

To find the total dose at point P it remains to add on the contribution due to the gas contained between the plates.

2.4 The Gas Contribution and the Total Absorbed Dose at a Point in the Gas

To find the gas contribution, refer to fig, 2.5. The circle marks the boundary of the equilibrium sphere while AA' and BB' are plane virtual interfaces located at the positions where the inside surfaces of the walls, now removed, would normally be situated. N_o electrons of energy E_o are assumed to be generated isotropically per unit volume in the gas so that the partial kerma, $\Delta K(E_o)$, equals $\frac{N_o E_o}{\rho}$.

The dose at P, which has been shown in section 2.1 to equal $\Delta K(E_o)$, may be thought of as the sum of the contributions from regions I, II and III. The contribution from region II, $\Delta D_g(x,E_o)$, is desired to complete the expression found in section 2.3. In terms of the geometrical factors,

$$\Delta K(E_o) = \Delta K(E_o)P(x,R_o) + \Delta D_g(x,E_o) + \Delta K(E_o)P(s-x,R_o).$$

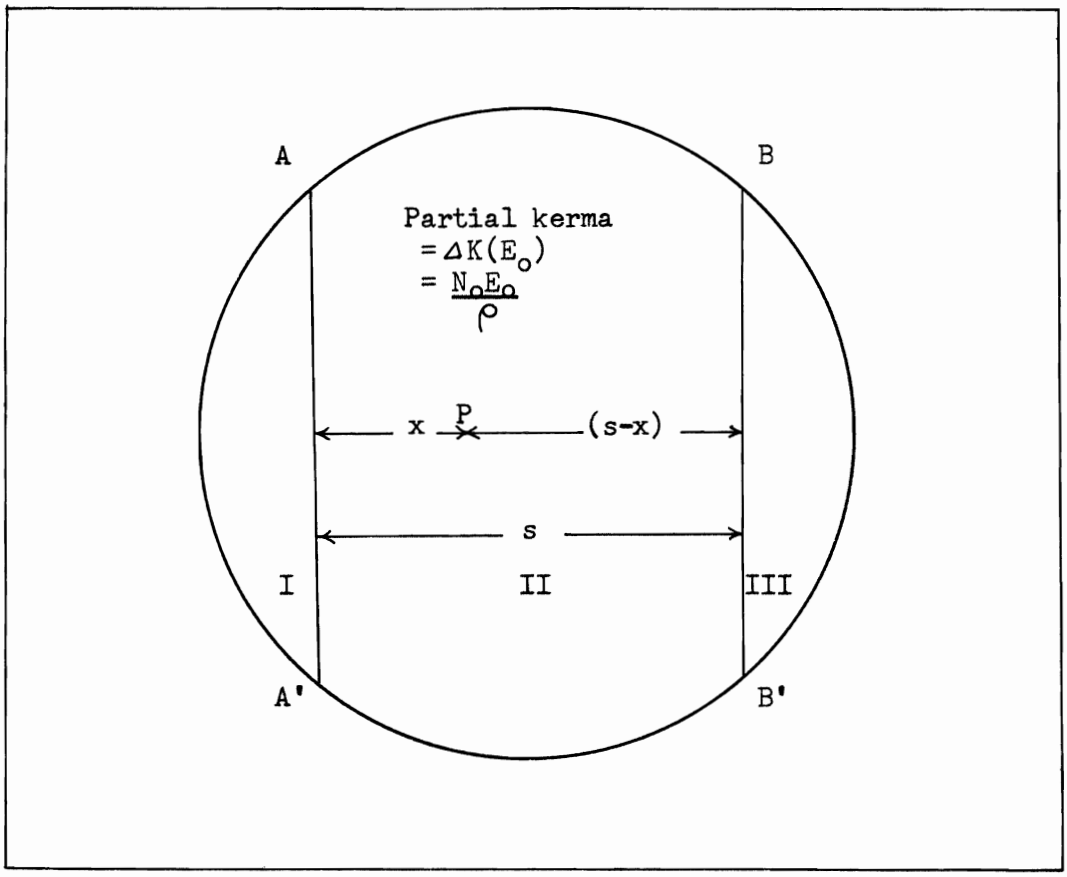

Figure 2.5 A diagram illustrating the geometry used to calculate the gas contribution to the total absorbed dose at point P.

Therefore,

$$\Delta D_g(x,E_o) = \Delta K(E_o)\cdot(1 - P(x,R_o) - P(s-x,R_o)) \qquad 2.11$$

or, for a spectrum of energies,

$$\Delta D_g(x) = \sum_{E_o} \Delta K(E_o)\cdot(1 - P(x,R_o) - P(s-x,R_o)). \qquad 2.12$$

Finally, the total absorbed dose, D(x), at P due to both walls and gas is given by,

$$D(x) = \sum_{E_o'} \frac{\Delta K'(E_o')}{n_m}\cdot P(x,R_o) + \sum_{E_o'} \frac{\Delta K'(E_o')}{n_m}\cdot P(s-x,R_o) + \sum_{E_o} \Delta K(E_o)\cdot(1 - P(x,R_o) - P(s-x,R_o)). \qquad 2.13$$

Equation 2.13 will be utilized in Chapter IV to calculate the absorbed dose theoretically.

As the plate separation approaches zero the geometrical factors approach their maximum values of 0.5 and equation 2.13 states that

$$D(0) = \sum_{E_o'} \frac{\Delta K'(E_o')}{n_m}.$$

This expression is equivalent to the Bragg-Gray relation given in section 1.2. The mass range ratio is approximately equivalent to the mass stopping power ratio, $(S/\rho)_m/(S/\rho)_g$, in the Bragg-Gray formula.

CHAPTER III

DETERMINATION OF THE X-RAY SPECTRUM

3.1 Introduction

To measure the X-ray spectrum, a NaI(Tl) crystal spectrometer, the calibration of which will be discussed in section 3.2, was employed (fig. 3.1). In this section will be given a qualitative description of the events taking place within the crystal and then within the photomultiplier tube when X-ray photons are incident on the crystal face. It will be shown how these events produce the distorted spectrum finally obtained from the multi-channel analyzer. The mathematical expression of the distortion will be the subject of sections 3.3 and 3.4.

Sodium iodide, when activated by a small amount of thallium (0.01 to 1 % by weight), becomes an excellent scintillator; i.e., when traversed by a charged particle such as an electron, it emits weak light flashes as the excited molecules return to the ground state. The main wavelength of emission has been found to be 4100 A. Moreover, the light output is proportional to the energy lost by the charged particle.

Suppose now that a narrow beam of monoenergetic photons of energy, say, 120 kev are perpendicularly incident on the crystal. A particular photon may interact with an electron within the scintillator by the photoelectric effect or the Compton effect. In the former case it is fair to assume that the ejected photoelectron will deposit all

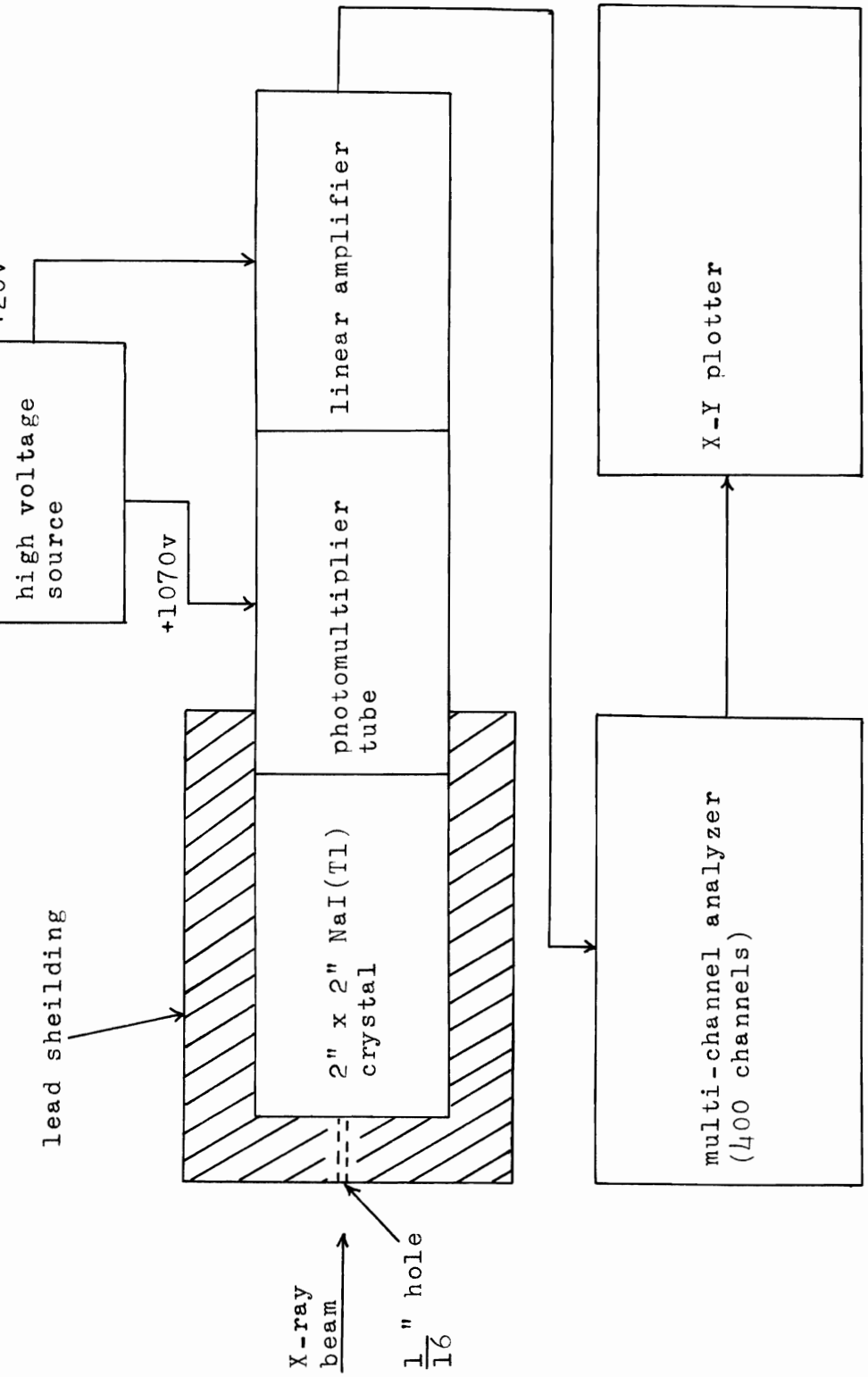

Figure 3.1 A block diagram illustrating the NaI(Tl) crystal spectrometer.

its energy in the crystal and so produce a light output proportional to the incident photon energy; in the Compton effect, however, the scattered photon may escape the crystal entirely with the result that the light output is charateristic of an (apparently) lower energy incident photon.

In addition, a special effect can occur when a 120 kev photon ejects an iodine K-shell electron and the X-ray then emitted escapes the detector. The ejected electron has an energy of 120 - 29 = 91 kev, where 29 kev is the energy of the K-shell of iodine, and, consequently, produces a light output characteristic of totally absorbed 91 kev incident photons. This is the origin of the "K escape-peak". Of course, the peak is not produced only by 120 kev photons, but can occur with any relatively low energy X- and gamma rays.

Figure 3.2 (parts A and B) summarizes the discussion so far.

The scintillations strike the cathode of the photomultiplier tube and liberate electrons. These electrons subsequently strike the several dynodes of the phototube, are greatly multiplied in number and finally produce voltage pulses at the photoanode. The pulses are further amplified by a linear amplifier and then analyzed according to their height and sorted in linear fashion by the multi-channel analyzer.

Evidently, the analyzer will not indicate a spectrum consisting only of a sharp line at one pulse height because of the situation depicted in fig. 2B. Furthermore, the spectrum will not have the shape indicated in fig. 2B because of additional distortion occurring in the phototube. To understand this new situation, suppose that an incident photon has ejected a photoelectron in the crystal and that

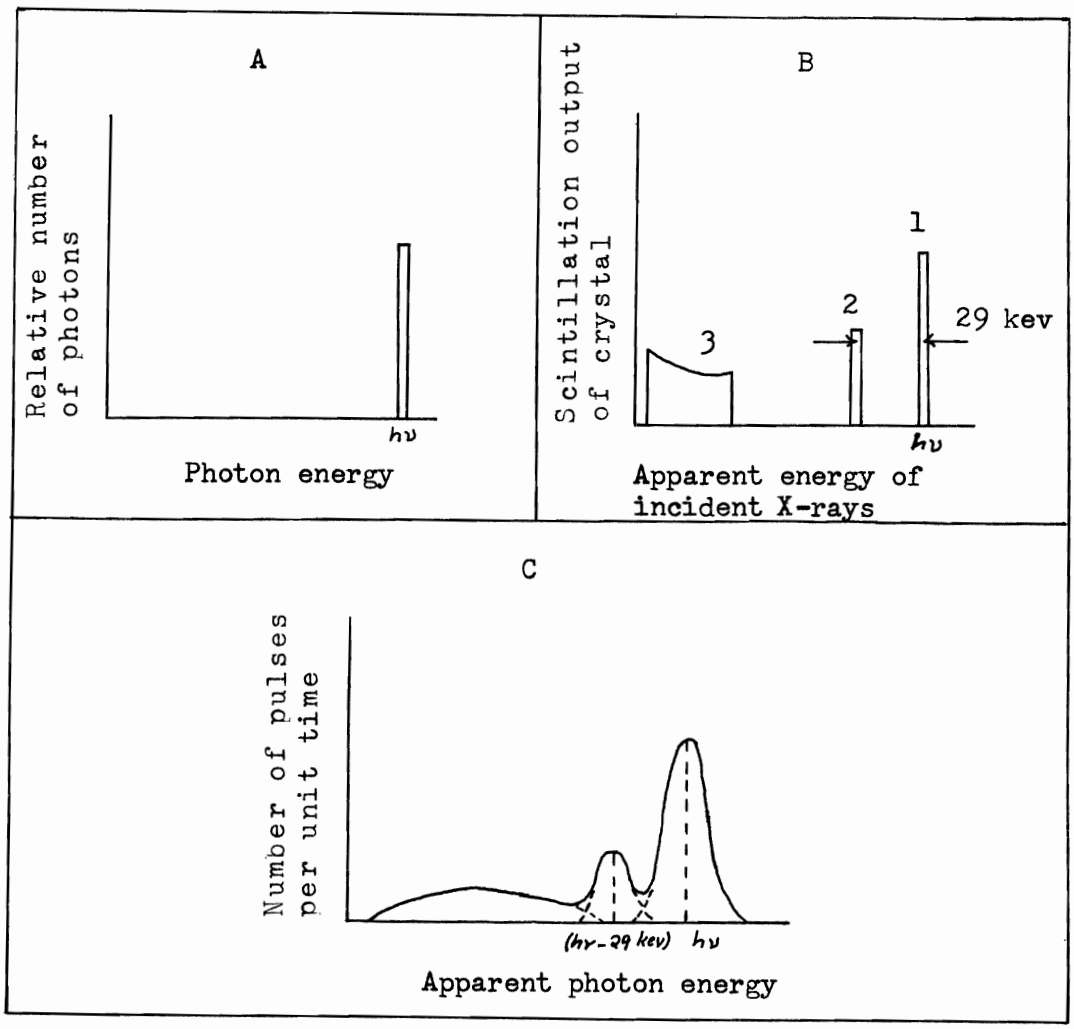

Figure 3.2 A typical scintillation distribution (part B) incident on the photomultiplier tube cathode when monoenergetic photons (part A) of energy hν = 120 kev, for example, strike the NaI(Tl) crystal. In 2B, part 1 arises from the photoelectric effect in which all the photon energy is deposited in the crystal, part 2 from the K escape effect and part 3 from the Compton effect in the crystal. Part C is discussed in the text.

this electron has deposited all its energy in the crystal. A second photon now arrives, undergoes the same interaction and leads to the same scintillation output. The two pulses finally appearing at the photoanode may not have the same height which, as explained by Skarsgard et al (1961), is a result of statistical fluctuations in the number of electrons reaching the photoanode, due mainly to fluctuations in the number of electrons emitted from the photocathode. The complete distribution of pulses has been found to follow very closely a Gaussian curve. Of course, the "Gaussian distortion" acts also on the Compton continuum and K escape line of fig. 2B.

Figure 3.2C is an illustration of the final spectrum, obtained from the analyzer, of incident photons of energy $h\nu$ = 120 kev, for example. The Gaussian shape of the main photopeak, centered at energy $h\nu$, and the K escape-peak, centered at energy ($h\nu$ - 29 kev), is clearly shown.

For photon energies below 100 kev the Compton interaction is unimportant and it is necessary to correct the measured spectrum only for K escape and Gaussian spread. This procedure was followed by Epp and Weiss (1966) in a very thorough study of primary diagnostic X-ray spectra with peak energies up to 105 kev.

The relative unimportance of the Compton interaction at low photon energies is well illustrated by the pulse height spectrum of the 47 kev gamma rays from Pb^{210} (fig. 3.3). Obtained with the spectrometer shown in fig. 3.1, the spectrum shows quite distinctly the Gaussian shapes of the photopeak, centered at 47 kev, and the K escape-peak, centered at 18 kev.

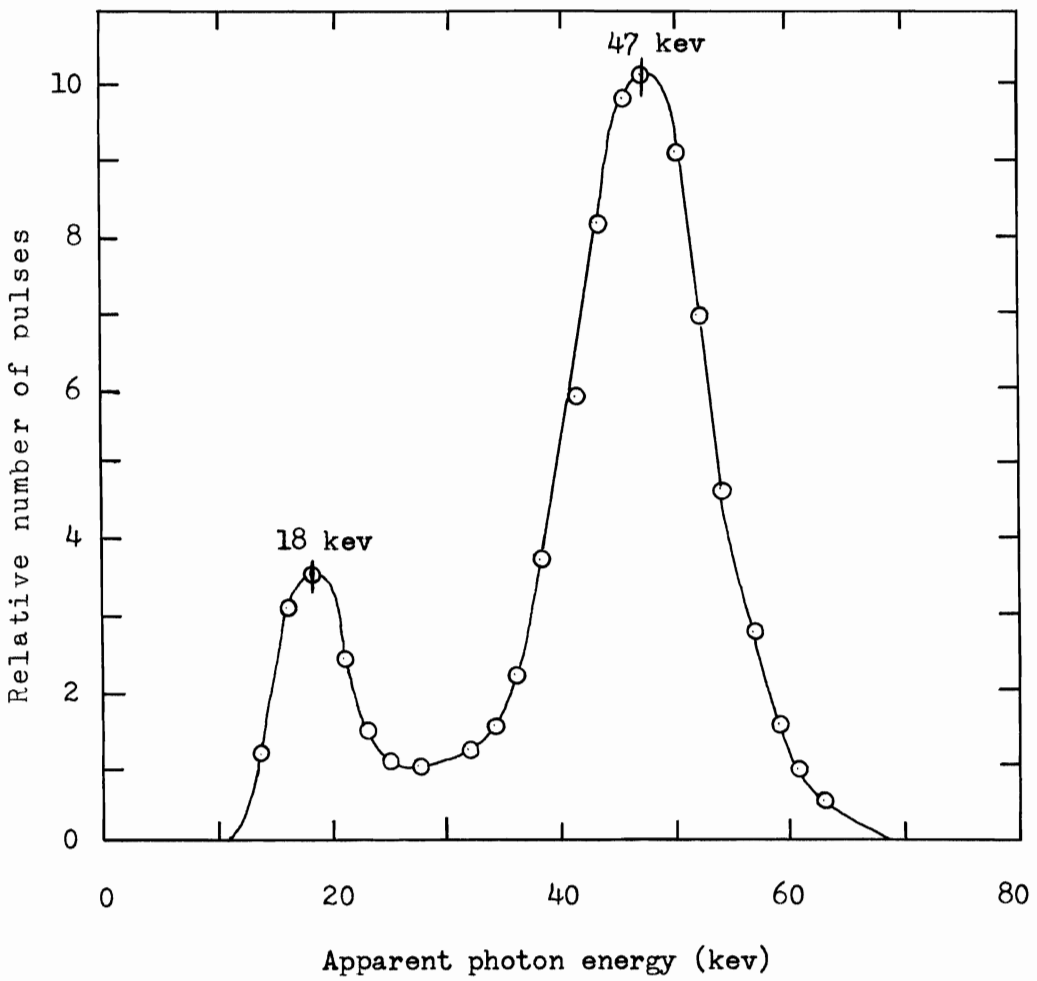

Figure 3.3 The pulse height spectrum of Pb^{210}.

3.2 Calibration of the Detecting System

Before the NaI(Tl) spectrometer can be used to measure unknown spectra, it is first calibrated with whatever monoenergetic gamma ray sources are available. The calibration amounts to finding the relation between the incident photon energy and channel number.

The sources used were Cs^{137} (662 kev and 32 kev), Co^{57} (123 kev) and Pb^{210} (47 kev). The K escape-peak of Pb^{210} at 18 kev was also suitable. In addition, a Compton effect setup was used with Cs^{137}. When the 662 kev gamma rays were allowed to strike an aluminum plate the scattered gamma rays at 70° (358 kev), 90° (289 kev) and 120° (225 kev) with respect to the initial beam direction provided the three additional calibration points given in parentheses. The channel number at the center of the photopeak (the center of the K escape-peak for the calibration point at 18 kev) was used to plot the calibration curve.

Where possible, the calibration was performed with the same geometry under which the final measurements are made, viz., with the $\frac{1}{16}$" diameter collimator. With the Pb^{210} source and the Compton setup this was not possible due to low counting rates. Fortunately, as can be seen from the calibration curve (fig. 3.4), all points fall along the same straight line so that the use of a larger diameter collimator does not introduce any significant error.

Another point deserving mention concerns the non-linear response of NaI(Tl). Several authors (for example, Epp and Weiss 1966, Skarsgard *et al* 1961) have found that the relationship between incident gamma ray energy and final pulse amplitude is not linear in the low energy region (from about 20 to 90 kev). The effect is small,

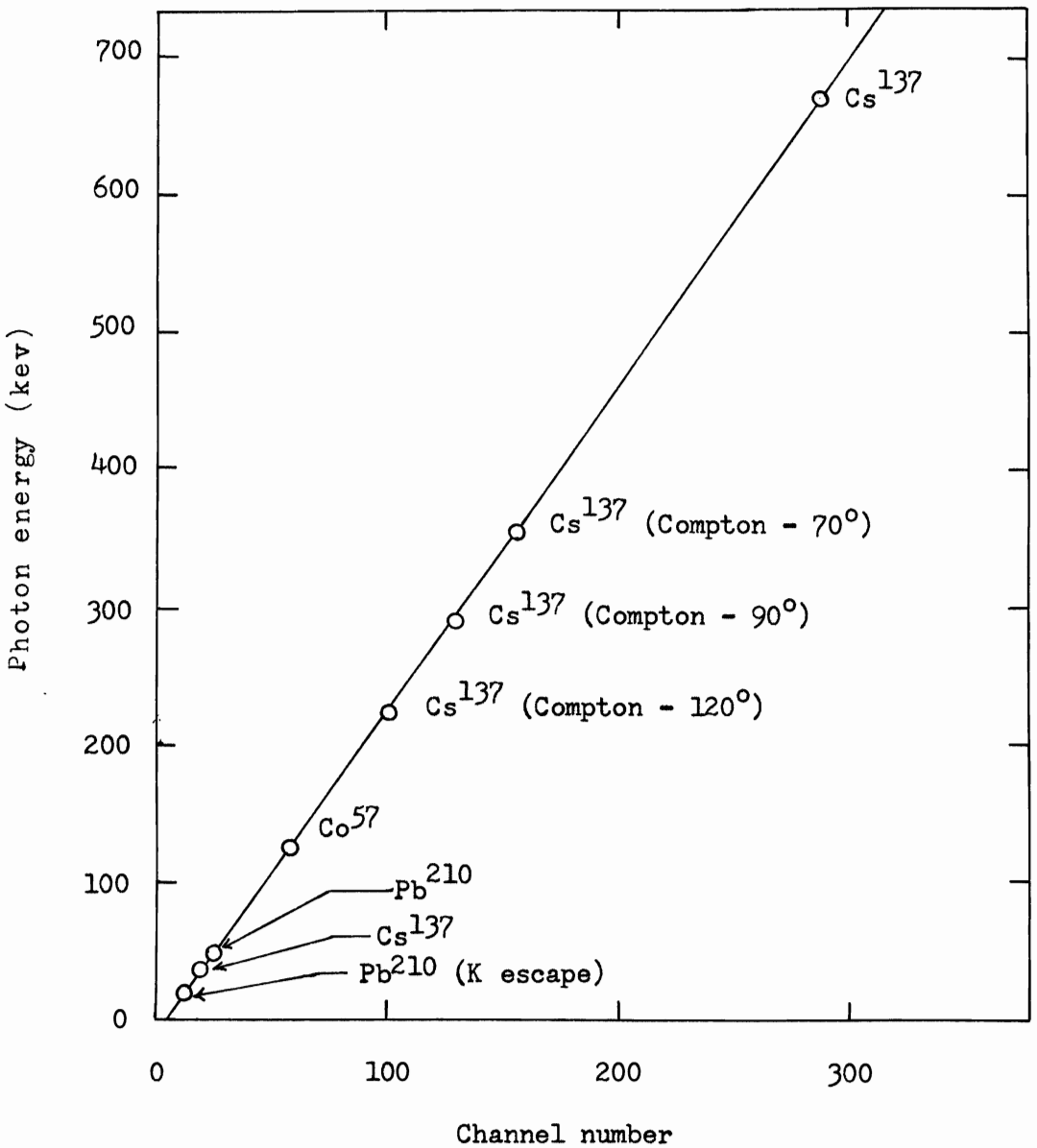

Figure 3.4 Spectrometer calibration curve.

however, and was not observed in the calibration of the spectrometer used in the present study.

3.3.1 The Mathematical Expression of the Gaussian Distortion

Following Skarsgard *et al* (1961), the correction for Gaussian spread was performed by using the formula

$$P(h\nu', h\nu) = N\exp(-(h\nu'-h\nu)^2K^2). \qquad 3.1$$

$P(h\nu', h\nu)$ is the probability of observing pulses corresponding to apparent photon energy $h\nu'$ when photons of energy $h\nu$ are incident, K is a characteristic of the detector and is a function of $h\nu$ and N is a normalization factor to be chosen so that

$$N\int_0^\infty \exp(-(h\nu'-h\nu)^2K^2)\, d(h\nu') = 1.$$

The value of N is readily found to be $N = \frac{K}{\sqrt{\pi}}$.

From equation 3.1 the width, W, of the Gaussian at half-maximum height is

$$W = \frac{2\sqrt{\ln 2}}{K}. \qquad 3.2$$

Experimentally, one finds that W is proportional to $h\nu^n$ where n varies from detector to detector. The resolution, Res., the ratio of W to $h\nu$, may then be expressed as

$$\text{Res.} = \frac{W}{h\nu} = C(h\nu)^{n-1}. \qquad 3.3$$

Using equations 3.2 and 3.3 the expression for K becomes

$$K = \frac{2\sqrt{\ln 2}}{C(h\nu)^n}$$

and the complete probability expression is

$$P(h\nu', h\nu) = \frac{2}{\sqrt{\pi}} \frac{\ln 2}{C(h\nu)^n} \exp\left[-(h\nu'-h\nu)^2 \frac{4 \ln 2}{C^2(h\nu)^{2n}}\right]. \qquad 3.4$$

The photopeak resolution for the 47, 123 and 662 kev gamma rays was measured and the results are given in fig. 3.5. A log-log plot of the data yields after a least squares fit the values C = 1.009 and n = 0.662. $P(h\nu', h\nu)$ was now evaluated with $h\nu', h\nu$ = 2,4,...,80 kev. The forty response vectors (one for each value of $h\nu$) were combined to form the 40 x 40 matrix, G, which constitutes the statistical (Gaussian) part of the detector response. The computer program in which G is formed and used is given in Appendix A.

3.3.2 The Mathematical Expression of the Escape of K X-rays

Evidently, if a sufficient number of monoenergetic sources are available, the correction for K escape can be made from the final measured spectrum by finding the ratio of the area under the K escape-peak to the total area under the spectrum and plotting a graph of the results. Otherwise, as is done in this study, the K escape-fraction must be calculated.

Following Shafroth (1967), it is assumed that a narrow beam of monoenergetic photons is incident on a semi-infinite sodium iodide crystal as shown in fig. 3.6. The assumption of a semi-infinite crystal simplifies the calculation and, as pointed out by Shafroth, the error between the calculated escape fraction and the value actually measured with a finite crystal is less than 2.5 % as long as the thickness of the finite crystal exceeds 3 mm. Also, the assumption of a narrow incident beam is applicable since the

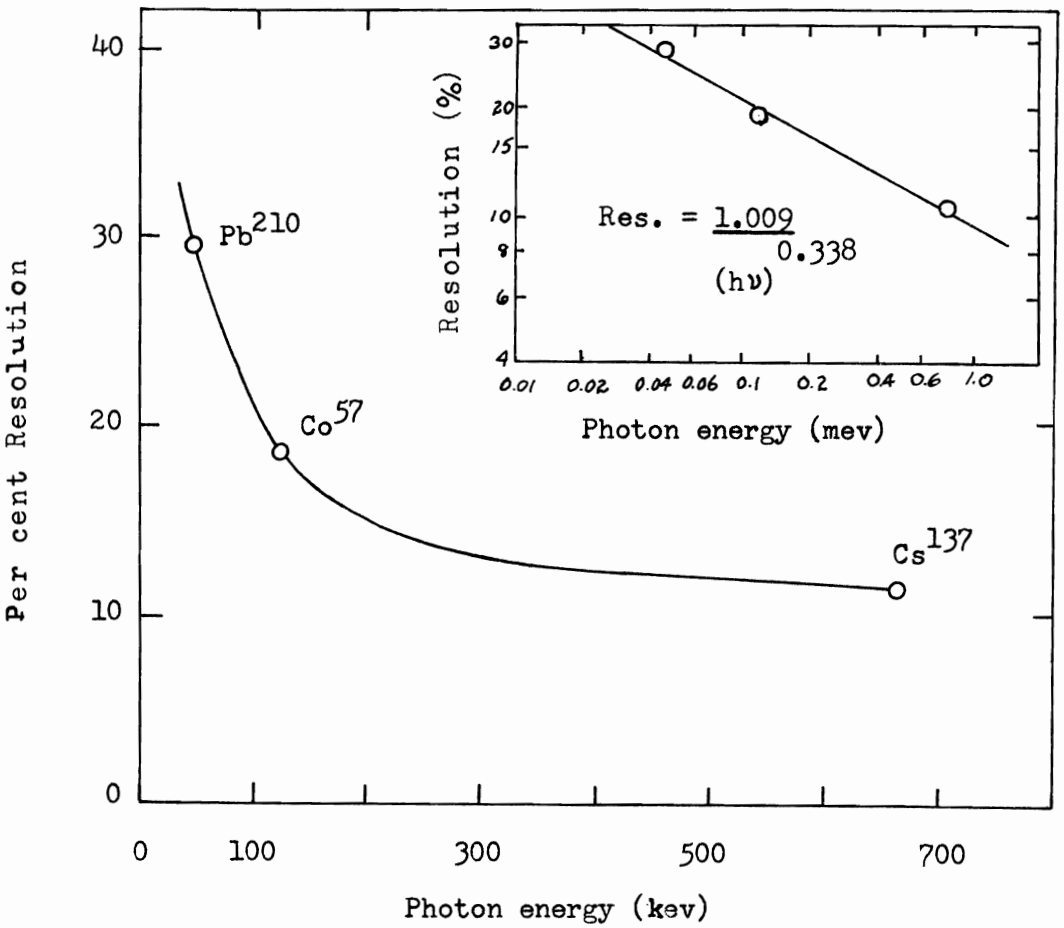

Figure 3.5 A graph of the resolution versus photon energy. The insert shows the data on a log-log plot from which the values of C and n are determined.

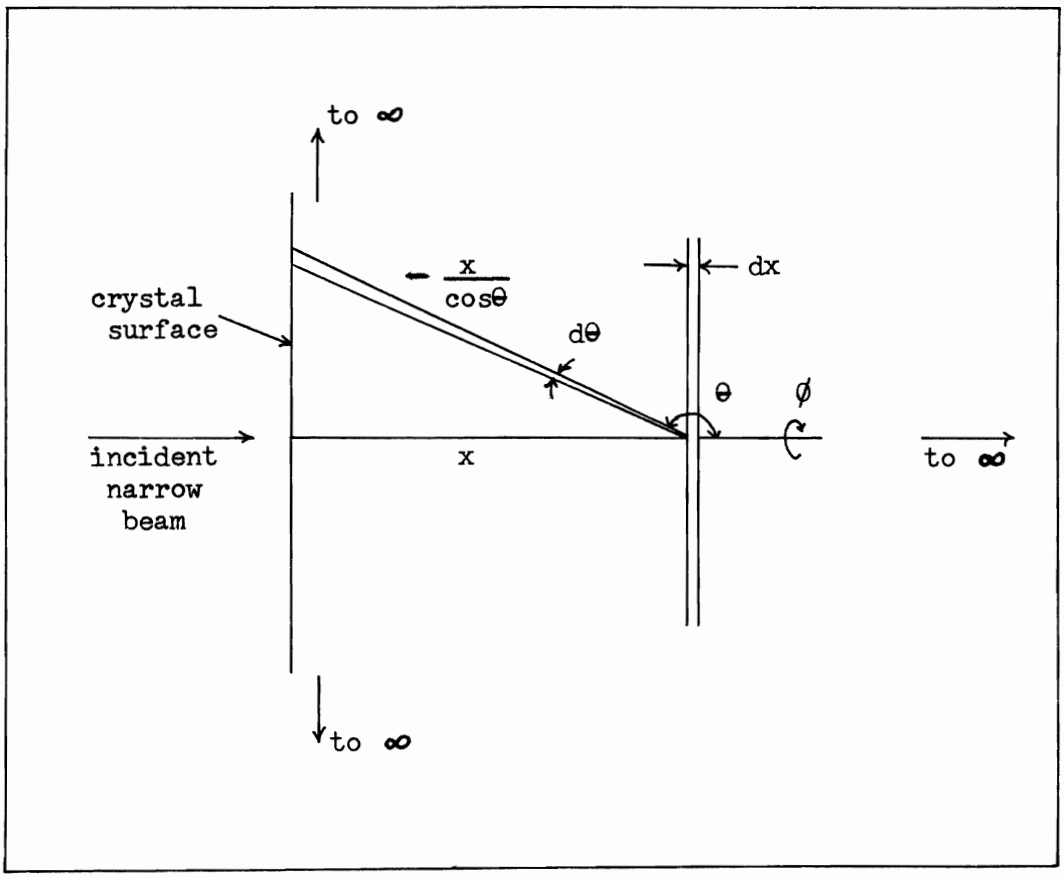

Figure 3.6 A diagram illustrating the geometry used to calculate the K escape-fraction.

spectrometer illustrated in fig. 3.1 uses a small collimator (1/16" in diameter).

Suppose now that N photons of energy $h\nu$ are normally incident on the crystal surface. $Ne^{-\mu_\gamma x}$ photons will reach layer dx at a distance x from the surface where μ_γ is the linear attenuation coefficient in sodium iodide for photons of energy $h\nu = \gamma$. The number of interactions then taking place in layer dx will be given by

$$Ne^{-\mu_\gamma x}\mu_\gamma dx.$$

Multiplying this by a factor $\frac{\tau_K}{\tau}$ (= 0.875) to take into account the relative contribution of the K shell to the photoelectric effect and a factor f_x (= 0.84) to account for the fact that sometimes no iodine K X-ray is produced, yields the number of iodine K X-rays from layer dx:

$$\frac{\tau_K}{\tau} f_x Ne^{-\mu_\gamma x}\mu_\gamma dx.$$

The number of X-rays starting out in solid angle $\sin\theta d\theta d\phi$ is just

$$\frac{\tau_K}{\tau} f_x Ne^{-\mu_\gamma x}\mu_\gamma dx \frac{\sin\theta d\theta d\phi}{4\pi}$$

and the number which finally escape through the crystal surface is

$$\frac{\tau_K}{\tau} f_x Ne^{-\mu_\gamma x}\mu_\gamma dx \frac{\sin\theta d\theta d\phi}{4\pi} e^{-\mu_x(-x/\cos\theta)}$$

where μ_x is the linear attenuation coefficient in sodium iodide for photons of energy 29 kev. Dividing by N and integrating gives the escape fraction, p_e:

$$p_e = \frac{\tau_K}{\tau} \frac{f_x}{4} \mu_\gamma \int_{\frac{\pi}{2}}^{\pi} \left(\int_0^{\infty} \left\{ \int_0^{2\pi} e^{\left[-\mu_\gamma + \frac{\mu_x}{\cos\theta}\right] x} \sin\theta \, d\phi \right\} dx \right) d\theta$$

$$p_e = \tfrac{1}{2} \mu_\gamma \frac{\tau_K}{\tau} f_x \int_{\frac{\pi}{2}}^{\pi} \left(\int_0^{\infty} e^{\left[-\mu_\gamma + \frac{\mu_x}{\cos\theta}\right] x} \sin\theta \, dx \right) d\theta \ .$$

The integration with respect to x is just:

$$\int_0^{\infty} e^{\left[-\mu_\gamma + \frac{\mu_x}{\cos\theta}\right] x} \, dx = \frac{1}{\left(-\mu_\gamma + \frac{\mu_x}{\cos\theta}\right)} \left[e^{\left(-\mu_\gamma + \frac{\mu_x}{\cos\theta}\right) x} \right]_0^{\infty}.$$

Since $\cos\theta$ is always negative, $\exp\left[-\mu_\gamma + \frac{\mu_\gamma}{\cos\theta}\right] x \Big|^{\infty} = 0$. Therefore,

$$\int_0^{\infty} e^{\left[-\mu_\gamma + \frac{\mu_x}{\cos\theta}\right] x} \, dx = - \frac{1}{\left[-\mu_\gamma + \frac{\mu_x}{\cos\theta}\right]} ,$$

and

$$p_e = \tfrac{1}{2} \mu_\gamma \frac{\tau_K}{\tau} f_x \int_{\frac{\pi}{2}}^{\pi} - \frac{\sin\theta}{\left[-\mu_\gamma + \frac{\mu_x}{\cos\theta}\right]} d\theta$$

$$p_e = \tfrac{1}{2} \mu_\gamma \frac{\tau_K}{\tau} f_x \int_{\frac{\pi}{2}}^{\pi} \frac{d(\cos\theta)}{\left[-\mu_\gamma + \frac{\mu_\gamma}{\cos\theta}\right]} .$$

Let $\cos\theta = Y$. Then,

$$p_e = \tfrac{1}{2} \mu_\gamma \frac{\tau_K}{\tau} f_x \int_0^{-1} \frac{dY}{\left[-\mu_\gamma + \frac{\mu_x}{Y}\right]}$$

$$= \tfrac{1}{2} \mu_\gamma \frac{\tau_K}{\tau} f_x \frac{1}{\mu_\gamma^2} \left[\mu_x - \mu_\gamma Y - \mu_x \ln \left| \mu_x - \mu_\gamma Y \right| \right]_0^{-1}$$

$$p_e = \tfrac{1}{2} \mu_\gamma \frac{\tau_K}{\tau} f_x \frac{1}{\mu_\gamma^2} \left[\mu_x + \mu_\gamma - \mu_x \ln (\mu_x + \mu_\gamma) - \mu_x + \mu_x \ln(\mu_x) \right].$$

Finally,

$$p_e = \tfrac{1}{2}\frac{\tau_K}{\tau} f_x\left[1 - \frac{\mu_x}{\mu_\gamma}\ln\left(1+\frac{\mu_\gamma}{\mu_x}\right)\right]$$

and substituting numerical values,

$$p_e = 0.367\left[1 - \frac{\mu_x}{\mu_\gamma}\ln\left(1+\frac{\mu_\gamma}{\mu_x}\right)\right]. \qquad 3.5$$

The K escape-fraction was evaluated from equation 3.5 using the values for μ given by Grodstein (1957) and the results are shown in fig. 3.7. The only experimental point (based on the 47 kev gamma ray from Pb^{210}) available is in fair agreement but it must be remembered that the Pb^{210} spectrum was not determined with the small collimator. The source actually subtended a sizeable half-angle, η, at the detector as shown in fig. 3.8. Under such circumstances the escape-fraction is greater and is, in fact, given by a formula presented by Shafroth but originally derived by Axel (1954):

$$p_e = \frac{0.367}{1-\cos\eta}\left[1 - \cos\eta - \frac{\mu_x}{\mu_\gamma}\cos^2\eta\,\ln\left(\frac{\mu_x}{\mu_\gamma}\cos\eta\right)\right.$$
$$+ \frac{\mu_x}{\mu_\gamma}\ln\frac{\mu_x}{\mu_\gamma} - \left(\frac{\mu_x}{\mu_x} - \frac{\mu_x}{\mu_\gamma}\cos^2\eta\right)\ln\left(\frac{\mu_x}{\mu_\gamma}\cos\eta + 1\right)$$
$$\left. + \left(\frac{\mu_x}{\mu_x} - \frac{\mu_x}{\mu_\gamma}\right)\ln\left(\frac{\mu_x}{\mu_\gamma} + 1\right)\right].$$

Using the escape-fraction data, another 40 x 40 matrix, EE, was constructed with a 2 kev interval (see Appendix A). The n^{th} column of EE refers to incident photons of energy $h\nu_n$ and has all zero elements except that element corresponding to energy $h\nu' = [h\nu_n - 29\text{ kev}]$, which has a value of $(p_e)_{h\nu_n}$, and that element corresponding to energy $h\nu' = h\nu_n$, which has a value of $(1 - p_e|_{h\nu_n})$.

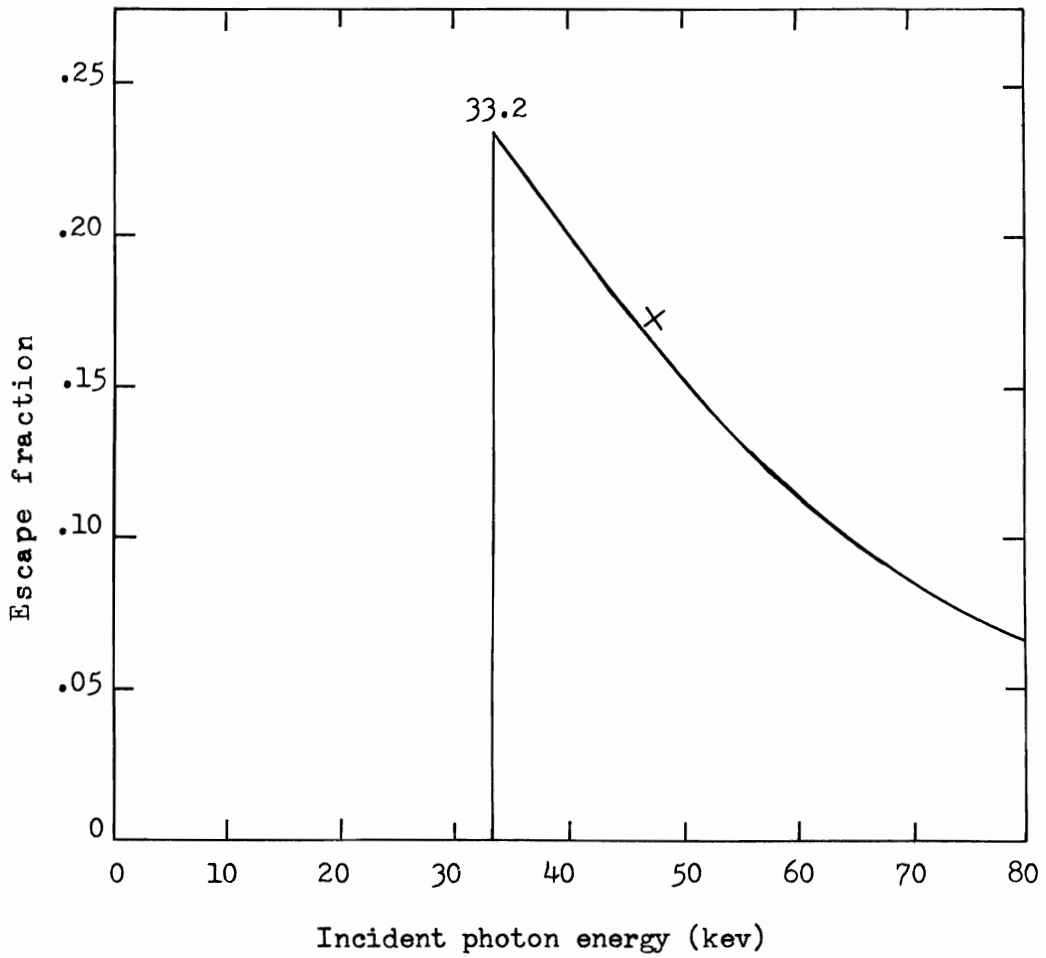

Figure 3.7 A graph of the K escape-fraction versus photon energy. The only experimental point, at 47 kev, is indicated by an "x".

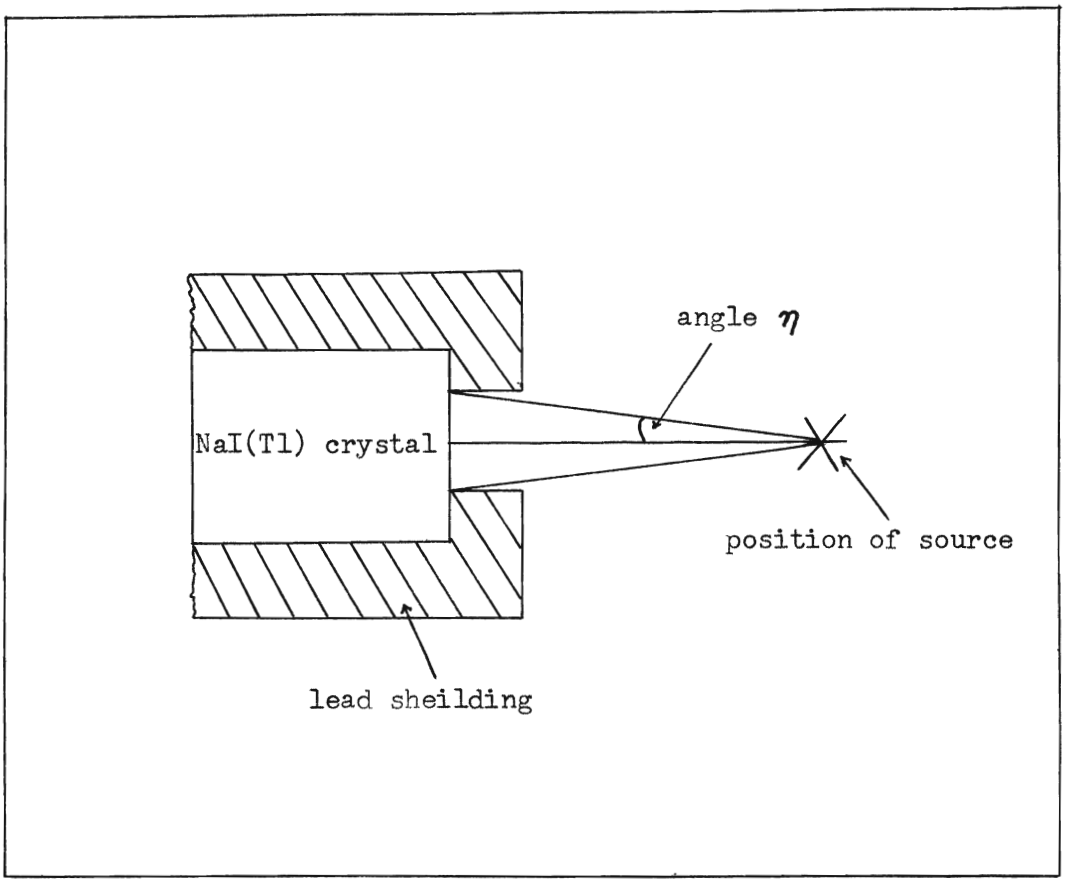

Figure 3.8 A diagram illustrating the geometry under which the Pb^{210} spectrum is measured.

Some difficulty is encountered since, for example, a 44 kev photon produces a K escape-peak centered at 15 kev which falls between the intervals centered at 14 and 16 kev. $p_e|_{h\nu_4}$ was thus divided up evenly into the two intervals.

It should be mentioned that the crystal efficiency factor,

$$1 - e^{-\mu L},$$

where L is the length of the crystal and μ is the linear attenuation coefficient for sodium iodide for photons of energy $h\nu$, has a value of unity in the range 2 to 80 kev. Thus, no correction is necessary for photons that pass through the crystal without interaction.

3.4 The Determination of the True X-ray Spectrum by Use of the Correction Matrices

Suppose that the ordinates (photons/cm^2) at energies 2,4,...,80 kev of a true incident spectrum are aligned to form a column matrix, I. Then EE•I represents the scintillation distribution incident on the photocathode and G(EE•I) = M the final measured spectrum. Clearly, one could perform the matrix multiplication, G•EE = C, so that M = CI and I = C^{-1}M. When using a small interval, however, it has been found that the inverted matrix, C^{-1}, is very sensitive to small errors in C and can "blow-up" (tend to have disproportionately large elements). Consequently, an alternative iterative method has come into favour. The method consists of guessing at I, forming CI and comparing the result with M. The iterations begin by assuming that I_o = M as a zero-order approximation. Thus, $CI_o = M_o$. One proceeds by setting $I_1 = I_o + (M-M_o)$ and so on so that in general, $I_n = I_o + (M-M_{n-1})$. Evidently, some criterion must be imposed to halt

the iterations. On the other hand, convergence to the true spectrum is very rapid. Freedman et al (1956) report that two to three iterations were sufficient to produce a calculated spectrum which was indistinguishable from the measured spectrum. Skarsgard et al found that four iterations were sufficient. Four iterations were found to be adequate in this study and fig. 3.9 shows the true spectrum, obtained after the fourth iteration. The spectrum is normalized to one roentgen and the measured spectrum, also normalized to one roentgen, is shown for comparison.

A Mueller MG 150/300 X-ray machine operating at 56 kvcp with minimum tube current and small focal spot was used to generate the X-ray spectrum. An aluminum filter, 1.03 mm thick, was used throughout the experiment and, since the spectrum between the plates of the ion chamber is desired (see Chapter II), a sheet of $\frac{1}{2}$" plexiglass and a piece of $\frac{1}{4}$" dural, the same thicknesses used in the chamber (fig. 4.1), were placed in front of the NaI(Tl) crystal. The crystal was located about ten feet from the exit port of the X-ray machine.

Using the formulas of section 1.3, the true X-ray spectrum was found to have an average energy of 36.6 kev, a H.V.T. of 2.4 mm Al and an effective energy of 30.4 kev. Mass attenuation coefficients necessary in the calculations were taken from Grodstein (1957) while mass energy transfer coefficients were taken from Berger (1961). Figure 3.10 is an experimental exposure transmission curve of the 56 kvcp spectrum measured with an Electronic Industries Limited (EIL) dosemeter. The H.V.T. is seen to be 2.6 mm Al, in reasonably good agreement with the calculated value.

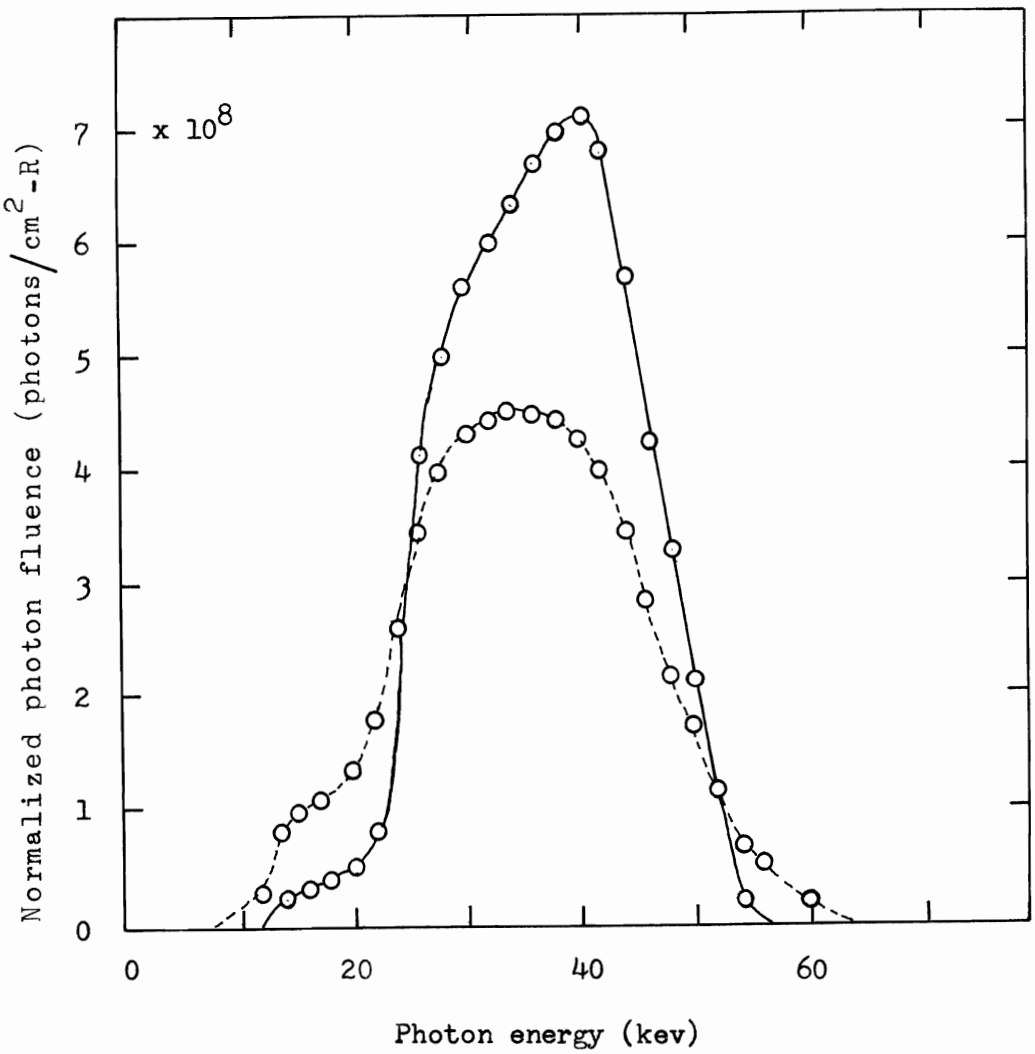

Figure 3.9 A comparison of the true 56 kvcp X-ray spectrum (solid line) and the measured spectrum (dotted line). Both spectra are normalized to 1R.

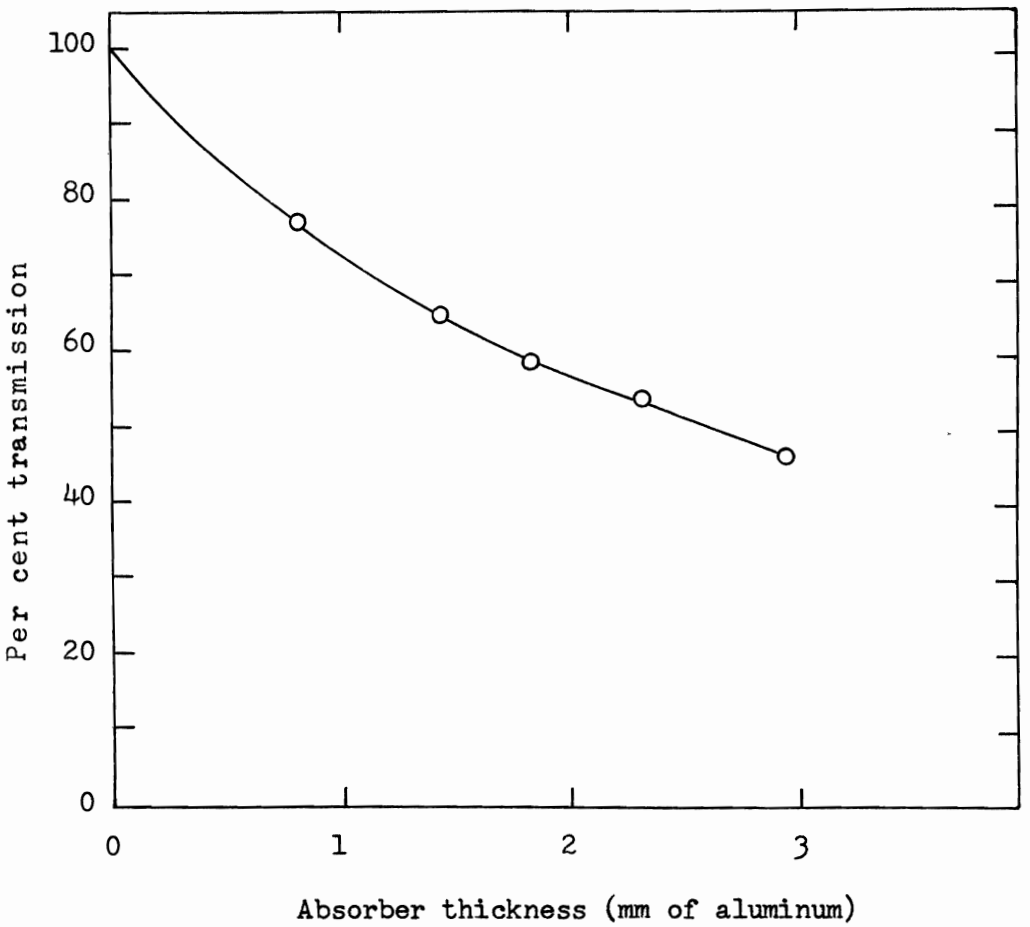

Figure 3.10 The experimental exposure transmission curve for the 56 kvcp X-ray spectrum.

Table 3.I is a tabulation of the normalized (1R) photon fluence, $\Delta\bar{\Phi}(h\nu)\cdot\Delta(h\nu)$, and the energy fluence. The energy fluence of photons of energy $h\nu$, $\Delta F(h\nu)$, is given by,

$$\Delta F(h\nu) = \Delta\bar{\Phi}(h\nu)\cdot h\nu\cdot\Delta(h\nu) \text{ ergs/cm}^2\text{-R}.$$

Note that $\Delta(h\nu) = 1$ kev. The energy fluence data will be used in Chapter IV to calculate the partial kermas in the walls and gas of the ion chamber.

It is evident that the X-ray spectrum determined above is that at the center of the beam. To investigate the shape of the beam off the central axis, a three-wheeled trolley on which the EIL dosemeter probe could be placed was constructed. By use of an electric motor, the trolley was drawn slowly across a table placed in front of the X-ray machine. The probe was connected to a Keithley model 605A electrometer the output of which was connected to a Texas Nuclear recorder. Figure 3.11 is the record of the "scan" made across the center of the beam. The beam falls off somewhat more quickly on one side but this is compensated by the slightly higher exposure rate on that side. The beam, then, is quite flat over the diameters of the chamber walls (fig. 4.1); this was also true of "scans" made both above and below the beam axis.

TABLE 3.I

NORMALIZED (1R) PHOTON FLUENCE AND ENERGY FLUENCE OF THE 56 KVCP SPECTRUM

Photon energy (kev)	Photon fluence (photons/cm^2-R)	Energy fluence (ergs/cm^2-R)
13	11.0×10^6	0.228
14	24.3	0.545
15	25.7	0.619
16	28.6	0.733
17	32.9	0.896
18	38.1	1.10
19	42.9	1.31
20	49.6	1.59
21	61.0	2.05
22	81.5	2.87
23	164	6.06
24	262	10.1
25	336	13.5
26	415	17.3
27	466	20.2
28	501	22.5
29	535	24.8
30	560	26.9
31	583	28.9
32	601	30.8
33	619	32.7
34	635	34.6
35	655	36.7
36	673	38.8
37	689	40.8
38	698	42.5
39	706	44.1
40	711	45.6
41	703	46.2
42	679	45.7
43	629	43.4
44	569	40.1
45	509	36.7
46	436	32.2
47	389	29.3
48	328	25.2
49	268	21.1
50	217	17.4
51	161	13.2
52	115	9.61
53	60.1	5.10
54	18.1	1.57
55	7.63	0.672
56	0	0

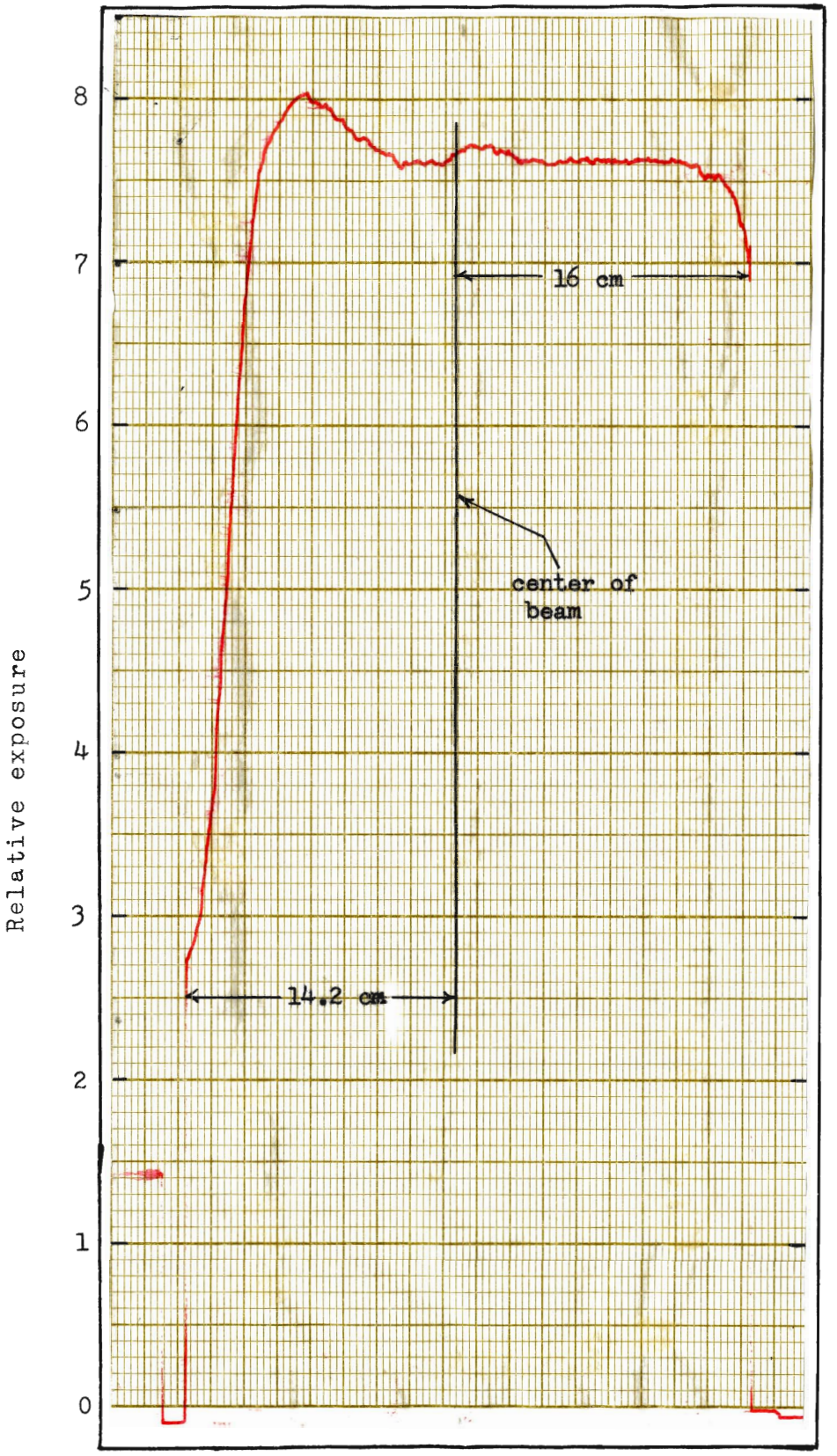

Figure 3.11 A "scan" made across the center of the X-ray beam with the EIL dosemeter.

CHAPTER IV

EXPERIMENTAL DETERMINATION OF ABSORBED DOSE IN AN ION CHAMBER: COMPARISON OF THEORY AND EXPERIMENT

4.1 Description of the Apparatus

The ionization chamber used in the experiment is shown in fig. 4.1. The parallel-plate chamber is of the guarded-field type with an electrically isolated collecting electrode of area 4.52 cm^2 centered in the back wall. The dural walls (see Table 4.V for the actual composition of the dural) are 29 cm in diameter and 0.64 cm thick. As the thickness is greater than the maximum energy electrons liberated in the plates by the 56 kvcp X-rays, no electrons from outside the chamber can ionize the gas between the plates.

An electrostatic field perpendicular to the plates in front of the collecting electrode defines the region from which ions are collected. The front plate can be moved back and forth by three micrometers. If s is the plate separation in centimeters then the mass, m, of air in the collecting volume is just,

$$m = 4.52\ (cm^2) \times s\ (cm) \times 0.001293\ (g/cm^3) \times \frac{p\ (torr)}{760\ (torr)} \times \frac{273}{273+t}\ g$$

where 0.001293 g/cm^3 is the density of air at 0 °C. and 760 torr, p is the gas pressure* and t is the room temperature in degrees

* measured with a Wallace and Tiernan absolute pressure gauge

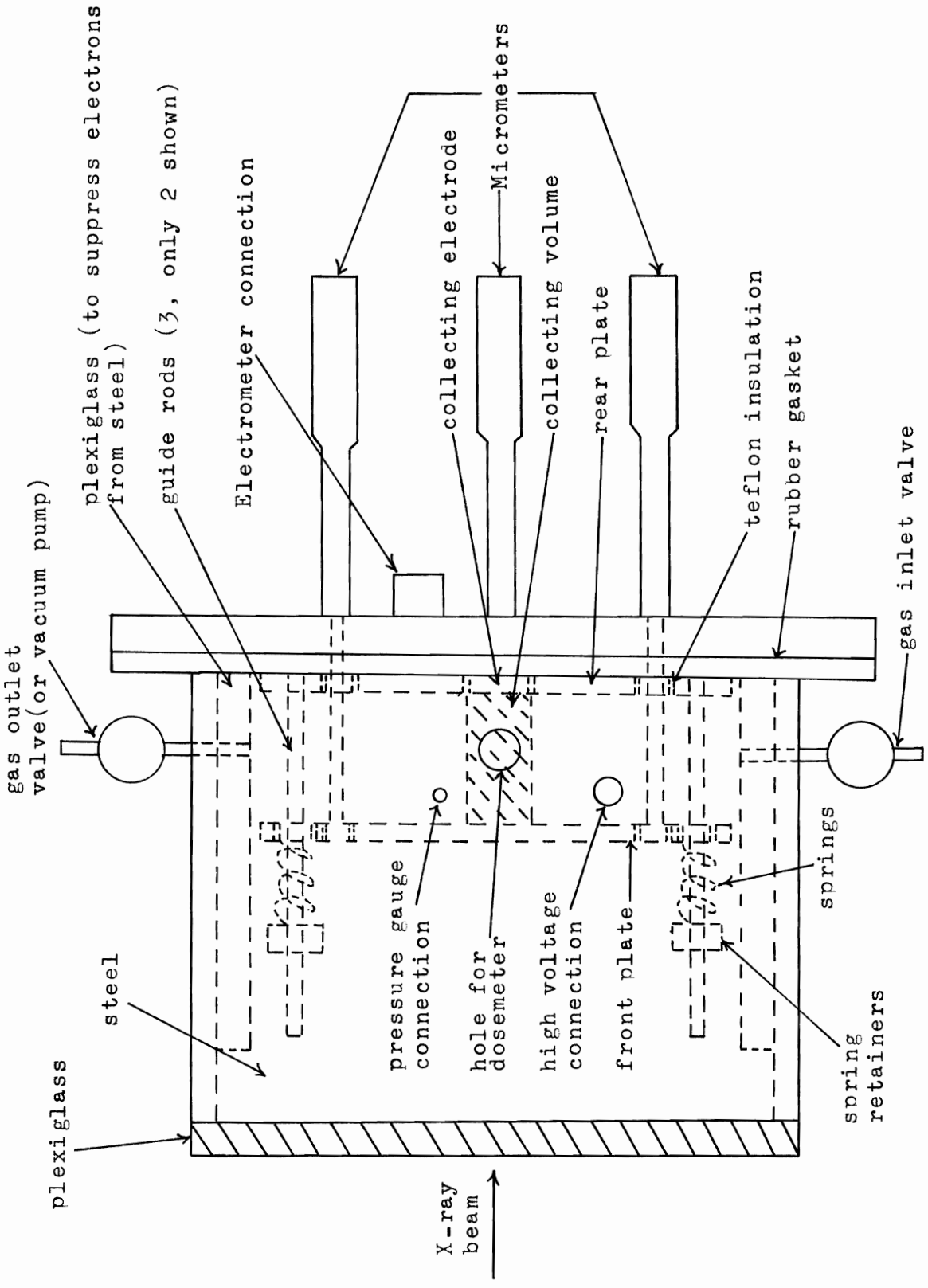

Figure 4.1 A simplified diagram (not to scale) of the ion chamber.

Centigrade.

The collecting electrode and guard area around the electrode are held at ground potential while a positive collecting voltage is applied to the front plate. The applied voltage was 70 volts in the plate separation range from 0 to 0.5 inches, 140 volts from 0.5 to 1.4 inches and 200 volts thereafter to the maximum plate separation of 1.9 inches. Measurements showed that these voltages were sufficient to permit collection of all ions.

The ion current was measured with a Keithley model 640 electrometer operating in the integrate mode. The current was permitted to charge a capacitor, C (= 20 pf in this case), contained within the electrometer to a voltage, V, in a certain time, T.

To compensate for small variations in the output of the X-ray machine all readings were monitored with a small parallel-plate ionization chamber fitted directly into the X-ray machine head. The output current of the monitor was fed into a dosemeter the scale readings of which were in "milliroentgens" (mR).

Details of the operation of the X-ray machine were identical to those which have been discussed in section 3.4.

4.2 Experimental Measurements

The experiment is performed by pumping the chamber to the selected gas pressure and fixing the desired plate separation. Chamber and monitor are exposed for the same period of time (two minutes) whereupon the capacitor voltage, V (volts), and the monitor reading, mR ("milliroentgens"), are taken. The plate separation is increased and the procedure then repeated. In this way, readings of $\frac{V}{mR}$

(volts/"mR") which are to be converted to absorbed dose per unit exposure are obtained. The variation with gas pressure and plate separation of the ratio $\frac{V}{mR}$ is shown in fig. 4.2.

Clearly, if the exposure is X (determined below) the absorbed dose per unit exposure, D_{air}^{Al}, is just,

$$D_{air}^{Al} = \frac{Q \text{ (coulombs)} \times 33.7 \text{ (ev/ion pair)} \times 1.602 \times 10^{-19} \text{ (ergs/ev)}}{1.602 \times 10^{-19} \text{ (coulombs/ion pair)} \times m \text{ (g)} \times X \text{ (roentgens)}} \qquad 4.1$$

where Q (= CV) is the total charge on capacitor C (= 20×10^{-12} farads) which has been charged to voltage V (volts) and m (grams) is the mass of the air in the collecting volume (see section 4.1).

The exposure is determined in three steps since, unfortunately, the Victoreen chambers, which give the exposure directly in roentgens, are not long enough to reach inside to the center of the chamber. First, a secondary standard ion chamber probe is placed between the plates of the ionization chamber. The output current of the probe is measured in the integrate mode by the Keithley electrometer. With the X-ray machine operating as in section 3.4 it was found that the ratio of the monitor reading to the capacitor voltage was,

$$\left[\frac{\text{"mR"}}{\text{volts}}\right]_1 = 103.8 \text{ "mR"/volt.}$$

In step two, the secondary probe is placed behind a $\frac{1}{4}$" piece of dural and a $\frac{1}{2}$" piece of plexiglass, the same thicknesses used in the chamber. The ratio of capacitor voltage to monitor reading was,

$$\left[\frac{\text{volts}}{\text{"mR"}}\right]_2 = 0.0103 \text{ volts/"mR".}$$

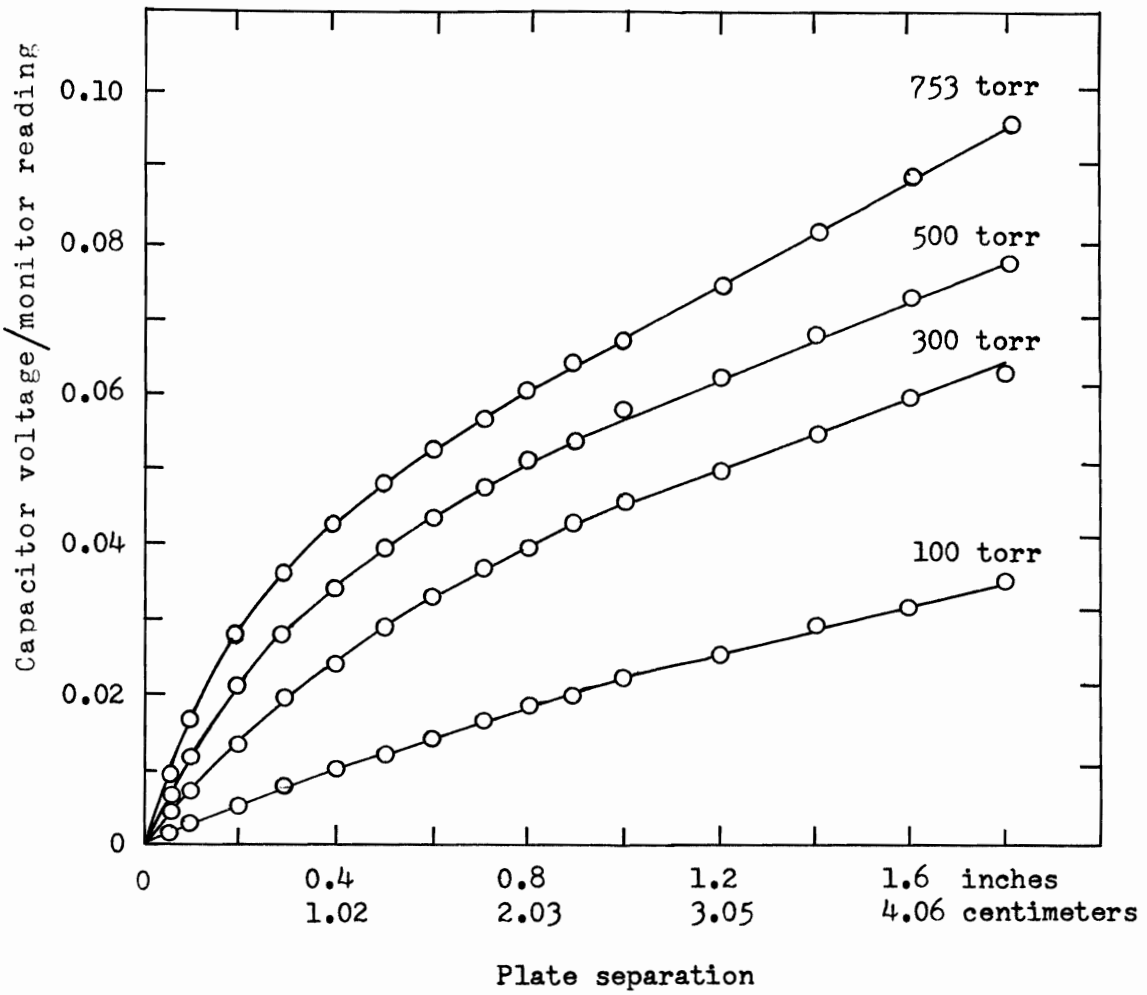

Figure 4.2 Variation with gas pressure and plate separation of the ratio of the capacitor voltage, V, to the monitor reading, mR.

In step three, the number 70-5, 25R chamber of the Victoreen model 570 condenser r-meter is substituted for the secondary probe behind the dural and plexiglass sheets. The ratio of the monitor reading to the number of roentgens was found to be,

$$\left[\frac{\text{"mR"}}{\text{R}}\right] = 4.748 \times 10^{3} \text{ "mR"/R.}$$

The Victoreen reading was corrected by a multiplicative factor equal to $\frac{760}{p}\,\frac{273+t}{295} = \frac{760}{755}\,\frac{273+22.6}{295} = 1.006$ since the pressure (p = 755 torr) and temperature (t = 22.6 °C.) differed from the conditions (760 torr and 22 °C.) at which the instrument reads correctly.

In the measurement of the exposure the dosemeter probes were placed at a distance of 85 cm from the X-ray machine target.

The final equation from which the absorbed dose per unit exposure in the gas can be calculated is now obtained from equation 4.1:

$$D^{Al}_{air} = \frac{C \times \frac{V}{mR} \times \left[\frac{\text{"mR"}}{\text{volts}}\right]_1 \times \left[\frac{\text{volts}}{\text{"mR"}}\right]_2 \times \left[\frac{\text{"mR"}}{\text{R}}\right] \times 33.7 \times 1.602 \times 10^{-12}}{1.602 \times 10^{-19} \times m}$$

$$= \frac{20 \times 10^{-12} \times \frac{V}{mR} \times 103.8 \times 0.0103 \times 4.748 \times 10^{3} \times 33.7 \times 1.602 \times 10^{-12}}{1.602 \times 10^{-19} \times 4.52 \times s \times 0.001293 \times \frac{p}{760} \times \frac{273}{273+t}}$$

$$D^{Al}_{air} = 16.3 \times 10^{3} \times \frac{V}{mR} \times \frac{273+t}{sp} \text{ ergs/g-R} \qquad 4.2$$

The experimental results, based on equation 4.2 and the measured values of $\frac{V}{mR}$, are given in Tables 4.I to 4.IV. Note that the values of temperature are slightly different since the data was taken on four different days.

One correction to the values of D^{Al}_{air} calculated from equation 4.2 is necessary since the exposure varies as the inverse square of the

TABLE 4.I

EXPERIMENTAL ABSORBED DOSE PER UNIT EXPOSURE AT A PRESSURE OF 753 TORR

$$D_{air}^{Al} = 16.3 \times 10^3 \times \frac{V}{mR}^{*} \times \frac{273+20}{s \times 753} \quad \text{(see equation 4.2)}$$

$$= \frac{6.35}{s} \times \frac{V}{mR} \times 10^3 \text{ ergs/g-R}$$

s (cm)	$\frac{V}{mR}$ $\left(\frac{\text{volts}}{\text{"mR"}}\right)$	D_{air}^{Al} $\left(\frac{\text{ergs}}{\text{g-R}}\right)$	$C(1/d^2)$ **	$D_{air}^{Al} \times C\left(\frac{1}{d^2}\right)$ $\left(\frac{\text{ergs}}{\text{g-R}}\right)$	s' *** (cm)
0.127	0.00944	471	1.053	496	0.118
0.254	0.0168	420	1.052	443	0.235
0.508	0.0275	344	1.050	361	0.470
0.762	0.0358	298	1.046	312	0.705
1.02	0.0422	264	1.043	276	0.940
1.27	0.0474	237	1.041	247	1.18
1.52	0.0520	216	1.038	224	1.41
1.78	0.0561	200	1.034	208	1.65
2.03	0.0602	188	1.031	194	1.88
2.29	0.0636	177	1.028	181	2.12
2.54	0.0670	168	1.025	172	2.35
3.05	0.0740	154	1.019	157	2.82
3.56	0.0811	145	1.012	147	3.29
4.06	0.0883	138	1.008	139	3.76
4.57	0.0955	133	1.001	133	4.24

* mR refers to reading of monitor dosemeter and is not a reading in milliroentgens

** see equation 4.3

*** see equation 4.4

TABLE 4.II

EXPERIMENTAL ABSORBED DOSE PER UNIT EXPOSURE AT A PRESSURE OF 500 TORR

$$D_{air}^{Al} = 16.3 \times 10^3 \times \frac{V}{mR}^{*} \times \frac{273+20}{s \times 500} \quad \text{(see equation 4.2)}$$

$$= \frac{9.58}{s} \times \frac{V}{mR} \times 10^3 \text{ ergs/g-R}$$

s (cm)	$\frac{V}{mR}$ $\left(\frac{\text{volts}}{\text{"mR"}}\right)$	D_{air}^{Al} $\left(\frac{\text{ergs}}{\text{g-R}}\right)$	$C(1/d^2)$**	$D_{air}^{Al} \times C$ $\left(\frac{\text{ergs}}{\text{g-R}}\right)$	s'*** (cm)
0.127	0.00642	482	1.053	509	0.078
0.254	0.0117	439	1.052	463	0.156
0.508	0.0211	396	1.050	416	0.312
0.762	0.0281	352	1.046	368	0.468
1.02	0.0339	318	1.043	338	0.624
1.27	0.0392	294	1.041	316	0.780
1.52	0.0436	273	1.038	283	0.935
1.78	0.0473	254	1.034	262	1.09
2.03	0.0511	240	1.031	248	1.25
2.29	0.0539	224	1.028	231	1.42
2.54	0.0575	216	1.025	221	1.56
3.05	0.0625	196	1.019	199	1.87
3.56	0.0679	183	1.012	185	2.18
4.06	0.0729	171	1.008	172	2.50
4.57	0.0776	162	1.001	162	2.81

* mR refers to reading of monitor dosemeter and is not a reading in true milliroentgens

** see equation 4.3

*** see equation 4.4

TABLE 4.III

EXPERIMENTAL ABSORBED DOSE PER UNIT EXPOSURE AT A PRESSURE OF 300 TORR

$$D_{air}^{Al} = 16.3 \times 10^3 \times \frac{V}{mR^*} \times \frac{273+19.3}{s \times 300} \quad \text{(see equation 4.2)}$$

$$= \frac{1.59}{s} \times \frac{V}{mR} \times 10^4 \text{ ergs/g-R}$$

s (cm)	$\frac{V}{mR}$ $\left(\frac{\text{volts}}{\text{"mR"}}\right)$	D_{air}^{Al} $\left(\frac{\text{ergs}}{\text{g-R}}\right)$	$C(1/d^2)$**	$D_{air}^{Al} \times C$ $\left(\frac{\text{ergs}}{\text{g-R}}\right)$	s'*** (cm)
0.127	0.00403	504	1.053	531	0.047
0.254	0.00768	480	1.052	505	0.094
0.508	0.0138	429	1.050	451	0.187
0.762	0.0197	410	1.046	428	0.280
1.02	0.0243	380	1.043	396	0.374
1.27	0.0290	362	1.041	378	0.468
1.52	0.0333	347	1.038	360	0.561
1.78	0.0368	328	1.034	350	0.654
2.03	0.0398	310	1.031	320	0.746
2.29	0.0428	297	1.028	304	0.841
2.54	0.0454	283	1.025	290	0.935
3.05	0.0502	262	1.019	266	1.12
3.56	0.0556	249	1.012	252	1.31
4.06	0.0595	232	1.008	234	1.50
4.57	0.0624	217	1.001	217	1.68

* mR refers to reading of monitor dosemeter and is not a reading in true milliroentgens

** see equation 4.3

*** see equation 4.4

TABLE 4.IV

EXPERIMENTAL ABSORBED DOSE PER UNIT EXPOSURE AT A PRESSURE OF 100 TORR

$$D_{air}^{Al} = 16.3 \times 10^3 \times \frac{V}{mR}^{*} \times \frac{273+20.7}{s \times 100} \quad \text{(see equation 4.2)}$$

$$= 4.76 \times \frac{V}{mR} \times 10^4 \text{ ergs/g-R}$$

s (cm)	$\frac{V}{mR}$ $(\frac{\text{volts}}{\text{"mR"}})$	D_{air}^{Al} $(\frac{\text{ergs}}{\text{g-R}})$	$C(1/d^2)$**	$D_{air}^{Al} \times C(\frac{1}{d^2})$ $(\frac{\text{ergs}}{\text{g-R}})$	s'*** (cm)
0.127	0.00152	570	1.053	601	0.016
0.254	0.00284	532	1.052	560	0.031
0.508	0.00547	512	1.050	538	0.062
0.762	0.00793	495	1.046	518	0.094
1.02	0.0102	478	1.043	499	0.124
1.27	0.0121	454	1.041	473	0.158
1.52	0.0142	444	1.038	461	0.187
1.78	0.0167	446	1.034	461	0.218
2.03	0.0186	435	1.031	448	0.249
2.29	0.203	423	1.028	434	0.280
2.54	0.0221	415	1.025	425	0.311
3.05	0.0257	402	1.019	409	0.374
3.56	0.0292	392	1.012	396	0.435
4.06	0.0319	374	1.008	376	0.498
4.57	0.0353	368	1.001	368	0.560

* mR refers to reading of monitor dosemeter and is not a reading in milliroentgens

** see equation 4.3

*** see equation 4.4

distance from the X-ray machine target. The correction assumes that the effective center for the production of electrons is at the center of the collecting volume. The effective center moves as the plate separation changes so that the correction factor, $C(1/d^2)$, is given by,

$$C(1/d^2) = \frac{(87.3 - s/2)^2}{85^2} \qquad 4.3$$

where s is the plate separation in centimeters. As has been mentioned, 85 cm is the distance from the X-ray machine target to the dosemeter probes. 87.3 cm is the distance of the front face of the back wall of the chamber from the X-ray machine target.

Charlton (1967) also made a correction for the fact that the theory of Chapter II assumes an infinitely large beam area whereas the plates of an ionization chamber have a finite area. The diameter of the plates of his chamber, however, were only 13 cm, less than half the diameter of the plates of the chamber used in this study. The correction for finite beam area would thus be entirely negligible in this case.

Another possible correction concerns the fact that the ionization current shows a small dependence upon the sign of the charge collected by the collecting electrode. This "polarity effect correction" is hardly significant since it amounts to only about 0.5 %.

The corrected values of the experimental absorbed dose per unit exposure are plotted in fig. 4.3 as a function of s', the equivalent plate separation at 0 °C. and 760 torr. s' is related to the indicated plate separation by,

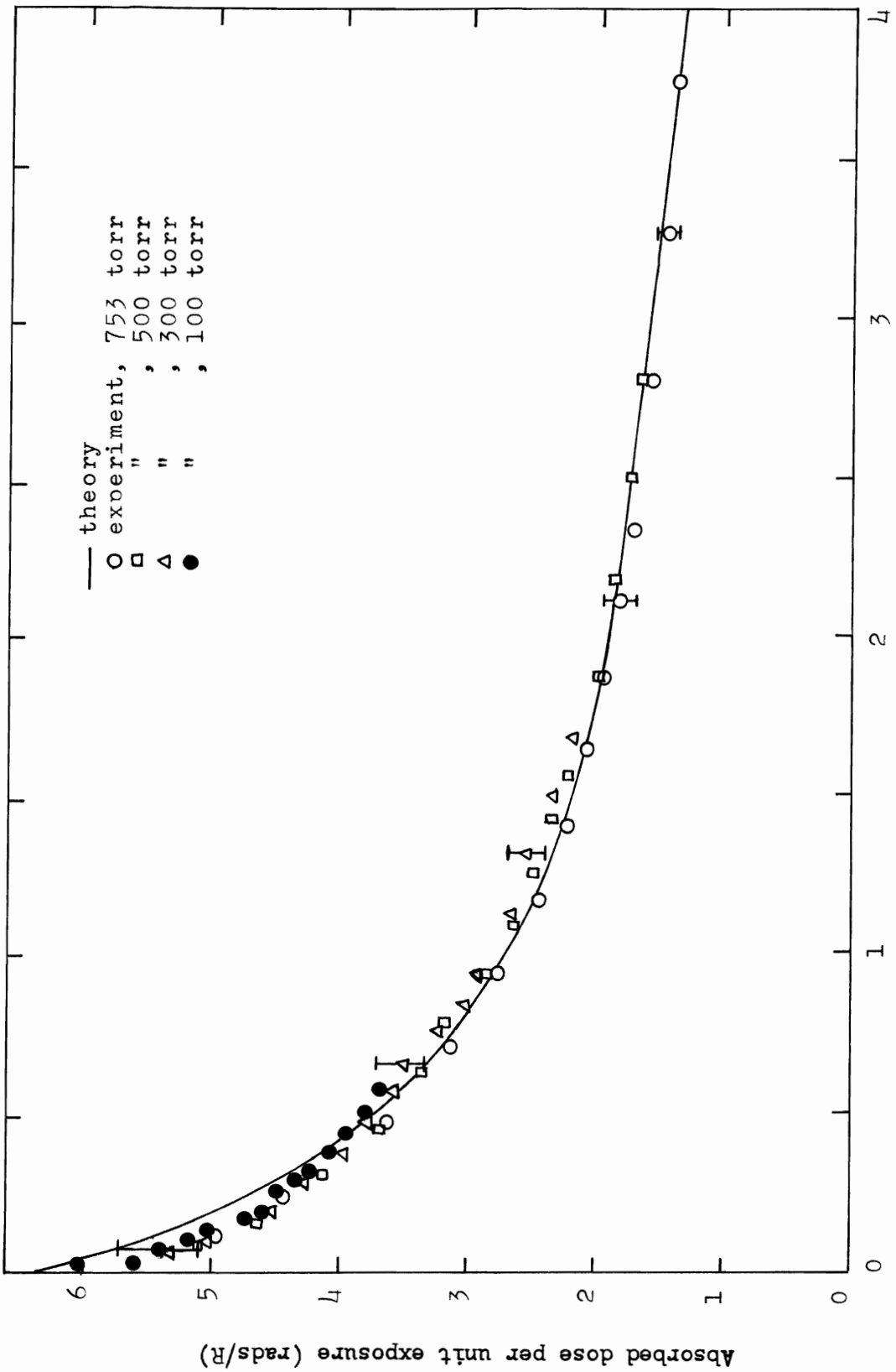

Figure 4.3 Absorbed dose per unit exposure as a function of equivalent plate separation. See Chapter V for estimates of the experimental error.

$$s' = s \times \frac{p}{760} \times \frac{273}{273+t}. \qquad 4.4$$

4.3 Theoretical Calculations

The solid line in fig. 4.3 is the theoretical curve based on equation 2.13.

The partial kermas necessary in equation 2.13 were evaluated by using the appropriate formulas given in section 1.2. Data on the Compton interaction was taken from Evans (1958) while all other data came from Berger (1961). In the case of air (75.5 % nitrogen, 23.2 % oxygen, 1.3 % argon by weight) data was taken directly from the two sources.

The dural walls of the ion chamber present a problem since, as seen from Table 4.V, the dural used has quite a complicated composition. Besides being very tedious, calculations to take into account each element present in the dural would probably not yield better information. Accordingly, a simplified composition was determined by use of the mass energy transfer coefficient, μ_K/ρ at 30 kev of the various elements. Berger has data tabulated at 30 kev and, furthermore, this energy is almost exactly the effective energy of the X-ray spectrum (see section 3.4).

Multiplying the assumed proportion by weight in which an element is present in the dural by its corresponding μ_K/ρ at 30 kev gives an idea of the relative importance of that element. $_{12}Mg$ and $_{14}Si$ were eliminated since the atomic number of aluminum (13) falls between their atomic numbers. Aluminum, then, has approximately the same effect as the two elements combined. For the remaining elements with atomic numbers between 22 and 30 the amount of iron necessary to

TABLE 4.V

COMPOSITION AS SUPPLIED BY THE MANUFACTURER OF THE 65ST DURAL USED FOR THE CHAMBER WALLS

Element	maximum % weight	assumed % weight	$\frac{\mu_K}{\rho}$ at 30 kev* (cm^2/g)	% weight x $\frac{\mu_K}{\rho}$ (cm^2/g)
$_{12}Mg$	0.8 - 1.2	1.00	0.698	0.70
$_{14}Si$	0.4 - 0.8	0.60	1.12	0.67
$_{22}Ti$	0.15	0.11	4.66	0.51
$_{24}Cr$	0.15 - 0.35	0.25	5.80	1.45
$_{25}Mn$	0.15	0.11	6.46	0.71
$_{26}Fe$	0.70	0.52	7.30	3.80
$_{29}Cu$	0.15 - 0.40	0.28	9.42	2.64
$_{30}Zn$	0.20	0.15	10.0	1.50
other	0.15			

Note: 1) Dural is composed mainly of aluminum. The substances listed above are other elements present in small amounts.

2) Where a range of % weight is given the mid-point of the range is used; if a single value is given the assumed % weight is 75 % of that single value.

* See the discussion in the text for the reason for using the mass energy transfer coefficient.

produce the same relative effect was calculated. Iron was chosen not only because its atomic number (26) falls at the mid-point of the range of the higher atomic number elements but also because it is the most abundant of these elements. Thus, a simplified dural composition of 98.5 % aluminum and 1.5 % iron was determined.

The remaining data, the c.s.d.a. electron ranges (see section 1.1), necessary in equation 2.13 was taken from Berger and Seltzer (1964). The computer program used in calculating the theoretical absorbed dose per unit exposure is given in Appendix A. Appendix B is a complete tabulation of the partial kermas.

CHAPTER V

DISCUSSION AND CONCLUSIONS

In view of the good agreement between theory and experiment over all plate separations (fig. 4.3) obtained in this study, the main conclusion is that the method due to Charlton and Cormack of calculating the absorbed dose distribution near an interface of two different materials undergoing X-ray irradiation may reliably be used at low photon energies.

It is very difficult to estimate the experimental errors. The plate separation is believed to be in error by a maximum of 5 % at 0.1 inches and less and by about 1 % at higher separations. The combined maximum possible error from all other sources (pressure, temperature, capacitor voltage, monitor reading, Victoreen dosemeter reading) is not expected to exceed 5 %.

It would be desirable to pay special attention to small plate separations (0.01 inch) and low gas pressures (50 torr) in order to check the agreement very near the interfaces. However, the experimental evidence of this thesis at the smallest equivalent plate separations would seem to suggest that no significant disagreement between the theory and experiment should be expected.

The Charlton-Cormack theory developed in Chapter II is not readily extended to high photon energies (recall that the model of electron range was stated to be applicable only up to 200 kev). Burlin (1966) has concluded, in fact, that in the energy range from

0.411 to 1.25 Mev the theory of Spencer and Attix (1955) is the best means of computing the energy absorbed in a medium from the ionization produced in a gas cavity. It would be of interest for further work, then, to apply the Spencer-Attix theory to low photon energies.

APPENDIX A

The two main programs used in this project are presented. PROGRAM SPECTRUM constructs the matrices G and EE according to section 3.3 and then forms the final correction matrix C = G•EE. C is then used to find the true X-ray spectrum by the iterative method given in section 3.4. PROGRAM CHAMBER calculates and averages the dose distribution inside the chamber according to equation 2.13. The partial kerma data used in CHAMBER is listed in APPENDIX B. The data on electron ranges was taken from Berger and Seltzer (1964).

```
      PROGRAM SPECTRUM
      DIMENSION EN(40),EE(40,40),P(40,40),T(40),TT(40),CM(40,40),H(40)
      READ(60,900) (T(N), N = 1,40)
  900 FORMAT(10F8.2/10F8.2/10F8.2/10F8.2)
   15 READ(60,1) I,Z,Y
    1 FORMAT(I3,F8.4,F6.1)
      EN(I) = Y
C     I is an index, EN the photon energy.  T (above) is the measured
C     spectrum, Z is the K escape-fraction.
      IF(EN(I)-34.0) 2,3,3
    2 DO 6 J = 1,40
      IF(J-I) 4,5,4
    5 EE(J,I) = 1.0000
      GO TO 6
    4 EE(J,I) = 0.0000
    6 CONTINUE
      GO TO 8
    3 II = (EN(I)-30.0)/2.0
      DO 7 J = 1,40
      IF(J-II) 9,10,9
   10 EE(J,I) = Z/2.
      EE(J+1,I) = Z/2.
      GO TO 7
    9 IF(J-II-1) 11,7,11
   11 IF(J-I) 12,13,12
   13 EE(J,I) = 1.0000 - Z
      GO TO 7
   12 EE(J,I) = 0.0000
```

```
    7 CONTINUE
    8 IF(I-40) 15,16,16
C     The above statements form the matrix EE.
   16 DO 100 J = 1,40
      U = EN(J)**.662
      V = 2.722/(EN(J)**1.324)
      DO 120 K = 1,40
      C = K
      D = C*2.0
      X = ABSF(D-EN(J))
      W = (X**2)*V
      IF(W-100.) 210,210,200
  200 W = 100.0000
  210 P(K,J) = .931/(U*EXP(W))
  120 CONTINUE
  100 CONTINUE
C     The above statements form the matrix P.
      DO 400 L = 1,40
      DO 405 M = 1,40
      CM(L,M) = 0.0000
      DO 410 N = 1,40
      CM(L,M) = CM(L,M) + P(L,N)*EE(N,M)
  410 CONTINUE
  405 CONTINUE
  400 CONTINUE
C     The above statements form the final correction matrix CM.
      WRITE(61,500)
  500 FORMAT(1H1,10X,23HFINAL CORRECTION MATRIX//)
```

```
      CALL MATRIX(CM)
C     MATRIX is a subroutine used to print out the final correction
C     matrix.  It may also be used to print EE and P.  The rest of
C     the program is concerned with the iterative method of
C     finding the true X-ray spectrum.  SUBROUTINE OUT prints the
C     final results.
      DO 1040 I = 1,40
 1040 H(I) = T(I)
      JEX = 1
C     JEX is an integer which limits the number of iterations to ten.
 1060 DO 700 M = 1,40
      TT(M) = 0.0000
C     H is the true spectrum, TT the measured spectrum.
      DO 705 N = 1,40
      TT(M) = TT(M) + CM(M,N)*H(N)
  705 CONTINUE
  700 CONTINUE
      DO 1000 K = 1,40
 1000 TT(K) = TT(K)*2.0000
      CALL OUT(JEX,EN,H,TT)
      JEX = JEX + 1
      IF(JEX.GT.10) 1400,1045
 1045 DO 1050 M = 1,40
 1050 H(M) = H(M) + (T(M)-TT(M))
      GO TO 1060
 1400 WRITE(61,1070)
 1070 FORMAT(1H0,10X,32HITERATION LIMIT HAS BEEN REACHED)
      STOP
```

```
      END

      SUBROUTINE MATRIX(A)
      DIMENSION A(40,40)
      DO 20 K = 1,40
      IF(K.EQ.11.OR.K.EQ.21.OR.K.EQ.31) 21,22
   22 WRITE(61,23) (A(K,L), L = 1,40)
   23 FORMAT(1H0,10X,10F8.4/11X,10F8.4/11X,10F8.4/11X,10F8.4)
      GO TO 20
   21 WRITE(61,24) (A(K,L), L = 1,40)
   24 FORMAT(1H1,10X,10F8.4/11X,10F8.4/11X,10F8.4/11X,10F8.4)
   20 CONTINUE
      RETURN
      END

      SUBROUTINE OUT (II,B,CC,DD)
      DIMENSION B(40),CC(40),DD(40)
      WRITE(61,1100) II
 1100 FORMAT(1H1,10X,19HITERATION NUMBER = ,I4//)
      WRITE(61,810)
  810 FORMAT(1H ,10X,11HENERGY(KEV),10X,14HTRUE(INCIDENT),10X,
     18HMEASURED//)
      DO 820 K = 1,40
      WRITE(61,830) B(K),CC(K),DD(K)
  830 FORMAT(1H ,10X,F11.1,10X,F14.4,5X,F13.4)
  820 CONTINUE
      RETURN
      END
```

```
      PROGRAM CHAMBER
      DIMENSION ALK(43),ALL(43),ALAUGER(43),ALCOMP(43),FEK(43),FEL(43)
      DIMENSION FEAUGER(43),FECOMP(43),GASK(43),GASL(43),GASAUGER(43)
      DIMENSION GASCOMP(43),P(101),RANALK(43),RANALL(43),RANALCOM(43)
      DIMENSION RANFEK(43),RANFEL(43),RANFECOM(43),RALGASK(43)
      DIMENSION RALGASL(43),RALGASCO(43),RFEGASK(43),RFEGASL(43)
      DIMENSION RGASK(43),RGASL(43),RGASCO(43),XX(100),ABSORB(100)
    2 READ(60,1) M,A1,A2,A3,A4,A5,A6,A7,A8
    1 FORMAT(I8,8F9.4)
      ALK(M) = A1
      ALL(M) = A2
      ALAUGER(M) = A3
      ALCOMP(M) = A4
      FEK(M) = A5
      FEL(M) = A6
      FEAUGER(M) = A7
      FECOMP(M) = A8
      IF(M-43) 2,6,6
    6 READ(60,5) J,C1,C2,C3,C4,C5,C6,C7
    5 FORMAT(I5,4F10.5,3E11.3)
      GASK(J) = C1
      GASL(J) = C2
      GASAUGER(J) = C3
      GASCOMP(J) = C4
C     ALK,.....GASCOMP is the partial kerma data in aluminum, iron
C     and air, respectively
```

```
      RGASK(J) = C5
      RGASL(J) = C6
      RGASCO(J) = C7
C     The ranges in air of the electrons liberated in air
      IF(J-43) 6,7,7
    7 READ(60,8) (P(L), L = 1,101)
C     The geometrical factor
    8 FORMAT(13F6.3/13F6.3/13F6.3/13F6.3/13F6.3/13F6.3/13F6.3/10F6.3)
      DO 9 K = 1,43
      READ(60,10) RANALK(K),RANALL(K),RANALCOM(K),RANFEK(K),RANFEL(K),RA
     1NFECOM(K)
C     The ranges in aluminum of the aluminum and iron electrons
   10 FORMAT(6E11.3)
    9 CONTINUE
      DO 11 J = 1,43
      READ(60,12) RALGASK(J),RALGASL(J),RALGASCO(J),RFEGASK(J),RFEGASL(J
     1)
C     The ranges in air of the aluminum and iron electrons
   12 FORMAT(5E11.3)
   11 CONTINUE
      RANALAUG = 5.300E-05
      RANFEAUG = 2.270E-04
C     The ranges in aluminum of the aluminum and iron Auger electrons
      RANGASAU = 1.000E-05
C     Range in the gas of the Auger electrons liberated in the gas.
C     For air, a dummy value is used since their is no Auger effect
      RALGASAU = 4.400E-05
```

```
      RFEGASAU = 1.880E-04
C     The ranges in air of the aluminum and iron Auger electrons
      DO 20 K = 1,100,10
C     In this DO loop, the dose distribution is calculated and averaged
C     for ten different plate separations
      C = K
      S = 0.01*C
C     S is the plate separation in centimeters
      WRITE(61,21) S
   21 FORMAT(1H1,5X,19HPLATE SEPARATION = ,F8.3,1X,2HCM)
      SS = S*.001293
C     SS is the plate separation in units of GM/CM**2
      WRITE(61,22)
   22 FORMAT(1H0,2(5X,27HDISTANCE FROM INTERFACE(CM),5X,23HABSORBED DOSE
     1(ERGS/G-R))/)
      DO 23 L = 1,100
C     This DO loop divides the plate separation by 100 and calculates
C     the dose at each of the 100 points.  These 100 values are averaged,
C     the average value being printed out as the absorbed dose for a
C     particular plate separation.  If the program is working properly
C     the loop need only go from L = 1,50 since the dose distribution
C     is symmetric
      D = L
      X = ((D-1.)*SS)/100.0
      XX(L) = X/.001293
      CALL DOSE(X,RGASK,P,SS,GASK,U1)
C     The contribution, U1, of the air photoelectrons to the absorbed dose
```

```
      CALL DOSE(X,RGASL,P,SS,GASL,U2)
C     The contribution, U2, of the gas L-shell photoelectrons. The
C     partial kerma for air is, of course, zero. The contribution
C     of the air photoelectrons is given by U1
      U3 = 0.0000000
C     U3 is the contribution of the gas Auger electrons. For air,
C     this contribution is zero
      W3 = X/(0.7*RANGASAU)
      IF(W3-1.00) 51,52,52
   51 MM3 = W3*100. + 1.
      GO TO 53
   52 MM3 = 100
   53 Q3 = P(MM3) - ((P(MM3)-P(MM3+1))*(W3-((MM3-1)*.01))/.01)
C     A linear interpolation for the geometrical factor
      W4 = (SS-X)/(0.7*RANGASAU)
      IF(W4-1.00) 54,55,55
   54 MM4 = W4*100. + 1.
      GO TO 56
   55 MM4 = 100
   56 Q4 = P(MM4) - ((P(MM4)-P(MM4+1))*(W4-((MM4-1)*.01))/.01)
      DO 57 J = 1,43
      U3 = U3 + GASAUGER(J)*(1.-Q3-Q4)
   57 CONTINUE
      CALL DOSE(X,RGASCO,P,SS,GASCOMP,U4)
C     The contribution, U4, of the air Compton electrons
      CALL WALLS(X,RANALK,RALGASK,P,SS,ALK,U5)
C     The contribution, U5, of the aluminum K photoelectrons
```

```
      CALL WALLS(X,RANALL,RALGASL,P,SS,ALL,U6)
C     U6 is the contribution of the aluminum L photoelectrons
      CALL AUELEC(X,RANALAUG,RALGASAU,P,SS,ALAUGER,U7)
C     U7 is the contribution of the aluminum Auger electrons
      CALL WALLS(X,RANALCOM,RALGASCO,P,SS,ALCOMP,U8)
C     U8 is the contribution of the aluminum Compton electrons
      CALL WALLS(X,RANFEK,RFEGASK,P,SS,FEK,U9)
C     U9 is the contribution of the iron K photoelectrons
      CALL WALLS(X,RANFEL,RFEGASL,P,SS,FEL,U10)
C     U10 is the contribution of the iron L photoelectrons
      CALL AUELEC(X,RANFEAUG,RFEGASAU,P,SS,FEAUGER,U11)
C     U11 is the contribution of the iron Auger electrons
      CALL WALLS(X,RANFECOM,RALGASCO,P,SS,FECOMP,U12)
C     The contribution of the iron Compton electrons
      ABSORB(L) = U1+U2+U3+U4+U5+U6+U7+U8+U9+U10+U11+U12
   23 CONTINUE
      ADDUP = 0.0000000
      DO 300 NN = 1,100
  300 ADDUP = ADDUP + ABSORB(NN)
      AVERAGE = ADDUP/100.
      DO 200 JJ = 1,50
      WRITE(61,210) XX(JJ),ABSORB(JJ),XX(JJ+50),ABSORB(JJ+50)
  210 FORMAT(1H ,2(17X,F15.8,13X,E15.4))
  200 CONTINUE
      WRITE(61,310) AVERAGE
  310 FORMAT(1H0,5X,10HAVERAGE = ,E15.7,1X,8HERGS/G-R)
   20 CONTINUE
```

```
      STOP
      END

      SUBROUTINE DOSE(A,B,C,D,E,F)
      DIMENSION B(43),C(101),E(43)
      F = 0.0000000
      DO 24 N = 1,43
      W1 = A/(0.7*B(N))
      IF(W1-1.00) 25,26,26
25    MM1 = W1*100. + 1.
      GO TO 27
26    MM1 = 100
27    Q1 = C(MM1) - ((C(MM1)-C(MM1+1))*(W1-((MM1-1)*.01))/.01)
      W2 = (D-A)/(0.7*B(N))
      IF(W2-1.00) 40,41,41
40    MM2 = W2*100. + 1.
      GO TO 42
41    MM2 = 100
42    Q2 = C(MM2) - ((C(MM2)-C(MM2+1))*(W2-((MM2-1)*.01))/.01)
      F = F + E(N)*(1.-Q1-Q2)
24    CONTINUE
      RETURN
      END

      SUBROUTINE WALLS(AA,BB,CC,DD,EE,FF,GG)
      DIMENSION BB(43),CC(43),DD(101),FF(43)
      GG = 0.0000000
```

```
      DO 60 M = 1,43
      W5 = AA/(0.7*CC(M))
      IF(W5-1.00) 65,66,66
65    MM5 = W5*100. + 1.
      GO TO 67
66    MM5 = 100
67    Q5 = DD(MM5) - ((DD(MM5)-DD(MM5+1))*(W5-((MM5-1)*.01))/.01)
      W6 = (EE-AA)/(0.7*CC(M))
      IF(W6-1.00) 70,71,71
70    MM6 = W6*100. + 1.
      GO TO 72
71    MM6 = 100
72    Q6 = DD(MM6) - ((DD(MM6)-DD(MM6+1))*(W6-((MM6-1.)*.01))/.01)
      ZZ = CC(M)/BB(M)
      GG = GG + (FF(M)*(Q5+Q6))/ZZ
60    CONTINUE
      RETURN
      END

      SUBROUTINE AUELEC(AAA,BBB,CCC,DDD,EEE,FFF,GGG)
      DIMENSION DDD(101),FFF(43)
      GGG = 0.0000000
      W7 = AAA/(0.7*CCC)
      IF(W7-1.00) 80,81,81
80    MM7 = W7*100. + 1.
      GO TO 82
81    MM7 = 100
```

```
 82 Q7 = DDD(MM7) - ((DDD(MM7)-DDD(MM7+1))*(W7-((MM7-1)*.01))/.01)
    W8 = (EEE-AAA)/(0.7*CCC)
    IF(W8-1.00) 90,91,91
 90 MM8 = W8*100. + 1.
    GO TO 92
 91 MM8 = 100
 92 Q8 = DDD(MM8) - ((DDD(MM8)-DDD(MM8+1))*(W8-((MM8-1)*.01))/.01)
    ZZZ = CCC/BBB
    DO 100 I = 1,43
100 GGG = GGG + (FFF(I)*(Q7+Q8))/ZZZ
    RETURN
    END
```

APPENDIX B

The following ten tables are a complete tabulation of the partial kerma in air and the chamber walls (a composite of 98.5 % aluminum, 1.5 % iron). The pertinent formulas are given in section 1.2. Data on the Compton interaction was taken from Evans (1958); all other data such as the mass energy transfer coefficients, etc. was taken from Berger (1961).

For aluminum, the following values were used: binding energy of the K shell, ϕ_K = 1.5 kev, binding energy of the L shell, ϕ_L = 0, average energy of the Auger electrons, $\bar{E}_K$ = 1.5 kev, fluorescent yield, F_K = 0.04.

For iron, the values used were: ϕ_K = 7 kev, ϕ_L = 0.8 kev, $\bar{E}_K$ = 6.5 kev, F_K = 0.308.

TABLE B.I

PARTIAL KERMA IN AIR DUE TO THE PHOTOELECTRIC EFFECT

$h\nu$ (kev)	$\frac{\mu_K}{\rho}$ (cm^2/g)	$\frac{\tau}{\rho}$ (cm^2/g)	E_o (kev)	$\Delta K(E_o)$ (ergs/g-R)
13	2.04	2.03	13	0.465
14	1.62	1.61	14	0.881
15	1.25	1.24	15	0.770
16	1.05	1.04	16	0.766
17	0.868	0.862	17	0.773
18	0.710	0.704	18	0.774
19	0.595	0.589	19	0.769
20	0.502	0.495	20	0.787
21	0.437	0.430	21	0.883
22	0.378	0.371	22	1.07
23	0.334	0.326	23	1.98
24	0.293	0.285	24	2.87
25	0.258	0.250	25	3.36
26	0.230	0.222	26	3.83
27	0.204	0.195	27	3.94
28	0.182	0.173	28	3.89
29	0.163	0.154	29	3.82
30	0.145	0.136	30	3.65
31	0.132	0.122	31	3.54
32	0.120	0.110	32	3.39
33	0.109	0.0989	33	3.24
34	0.0995	0.0892	34	3.09
35	0.0908	0.0803	35	2.95
36	0.0838	0.0731	36	2.84
37	0.0775	0.0665	37	2.71
38	0.0717	0.0605	38	2.57
39	0.0665	0.0551	39	2.43
40	0.0622	0.0506	40	2.31
41	0.0580	0.0462	41	2.13
42	0.0544	0.0424	42	1.94
43	0.0512	0.0389	43	1.69
44	0.0484	0.0359	44	1.44
45	0.0461	0.0335	45	1.23
46	0.0440	0.0312	46	1.00
47	0.0420	0.0290	47	0.850
48	0.0402	0.0269	48	0.679
49	0.0389	0.0255	49	0.537
50	0.0376	0.0240	50	0.417
51	0.0364	0.0226	51	0.298
52	0.0352	0.0212	52	0.204
53	0.0342	0.0200	53	0.102
54	0.0333	0.0190	54	0.0298
55	0.0324	0.0179	55	0.0120

TABLE B.II

PARTIAL KERMA IN AIR DUE TO THE COMPTON EFFECT

$h\nu$ (kev)	$\frac{\sigma}{\rho} f_c$ (cm^2/g)	$\bar{E}_o$ (kev)	$\Delta K(\bar{E}_o)$ (ergs/g-R)
13	0.00460	0.31	0.00110
14	0.00490	0.36	0.00270
15	0.00520	0.40	0.00320
16	0.00550	0.46	0.00400
17	0.00580	0.52	0.00520
18	0.00610	0.58	0.00670
19	0.00640	0.64	0.00840
20	0.00670	0.70	0.0106
21	0.00700	0.78	0.0144
22	0.00730	0.85	0.0210
23	0.00760	0.94	0.0461
24	0.00790	1.02	0.0797
25	0.00810	1.11	0.109
26	0.00840	1.20	0.145
27	0.00860	1.30	0.174
28	0.00890	1.38	0.200
29	0.00910	1.50	0.226
30	0.00940	1.60	0.253
31	0.00960	1.68	0.279
32	0.00980	1.80	0.302
33	0.0101	1.90	0.331
34	0.0103	2.01	0.356
35	0.0105	2.12	0.386
36	0.0107	2.23	0.416
37	0.0110	2.35	0.449
38	0.0112	2.46	0.476
39	0.0114	2.58	0.503
40	0.0116	2.70	0.528
41	0.0118	2.82	0.545
42	0.0120	2.94	0.549
43	0.0123	3.06	0.533
44	0.0125	3.19	0.501
45	0.0126	3.32	0.463
46	0.0128	3.46	0.412
47	0.0130	3.58	0.381
48	0.0133	3.73	0.336
49	0.0134	3.86	0.282
50	0.0136	4.00	0.236
51	0.0138	4.15	0.182
52	0.0140	4.31	0.135
53	0.0142	4.47	0.0724
54	0.0143	4.62	0.0224
55	0.0145	4.78	0.00970

TABLE B.III

PARTIAL KERMA IN ALUMINUM DUE TO THE K-SHELL PHOTOELECTRIC EFFECT

$h\nu$ (kev)	$\frac{\tau_K}{\rho}$ (cm^2/g)	$(1-\phi_K/h\nu) = f_\tau^K$	$\frac{\tau_K f_\tau^K}{\rho}$ (cm^2/g)	E_o' (kev)	$\Delta K(E_o')$ x 0.985 (ergs/g-R)
13	11.2	0.885	9.92	11.5	2.23
14	8.72	0.893	7.77	12.5	4.18
15	6.70	0.900	6.03	13.5	3.68
16	5.60	0.906	5.07	14.5	3.66
17	4.39	0.912	4.01	15.5	3.54
18	3.78	0.917	3.47	16.5	3.76
19	3.16	0.921	2.91	17.5	3.75
20	2.71	0.925	2.51	18.5	3.93
21	2.33	0.929	2.26	19.5	4.57
22	2.01	0.932	1.87	20.5	5.30
23	1.76	0.935	1.65	21.5	9.85
24	1.53	0.937	1.43	22.5	14.2
25	1.35	0.940	1.27	23.5	16.8
26	1.19	0.942	1.12	24.5	19.1
27	1.06	0.944	1.00	25.5	19.9
28	0.945	0.946	0.895	26.5	19.8
29	0.844	0.948	0.800	27.5	19.6
30	0.753	0.950	0.715	28.5	19.0
31	0.690	0.952	0.656	29.5	18.7
32	0.624	0.953	0.594	30.5	18.0
33	0.567	0.955	0.541	31.5	17.5
34	0.518	0.956	0.496	32.5	16.9
35	0.472	0.957	0.452	33.5	16.4
36	0.430	0.958	0.422	34.5	16.1
37	0.394	0.959	0.378	35.5	15.2
38	0.360	0.961	0.346	36.5	14.5
39	0.331	0.962	0.318	37.5	13.8
40	0.305	0.963	0.294	38.5	13.2
41	0.281	0.963	0.270	39.5	12.3
42	0.259	0.964	0.247	40.5	11.1
43	0.239	0.965	0.231	41.5	9.87
44	0.221	0.966	0.214	42.5	8.46
45	0.206	0.967	0.199	43.5	7.20
46	0.191	0.967	0.185	44.5	5.86
47	0.178	0.968	0.172	45.5	4.97
48	0.167	0.969	0.162	46.5	4.03
49	0.155	0.969	0.150	47.5	3.11
50	0.146	0.970	0.142	48.5	2.43
51	0.137	0.971	0.134	49.5	1.74
52	0.129	0.971	0.125	50.5	1.18
53	0.120	0.972	0.117	51.5	0.588
54	0.112	0.972	0.109	52.5	0.168
55	0.104	0.973	0.101	53.5	0.0669

TABLE B.IV

PARTIAL KERMA IN ALUMINUM DUE TO THE L-SHELL PHOTOELECTRIC EFFECT

$h\nu$ (kev)	$\frac{\mu_K}{\rho}$ (cm^2/g)	$\frac{\tau_L f_\tau^L}{\rho}$ (cm^2/g)	E_o' (kev)	$\Delta K(E_o')$ x 0.985 (ergs/g-R)
13	11.9	0.735	13	0.165
14	9.46	0.786	14	0.423
15	7.48	0.801	15	0.488
16	6.15	0.571	16	0.412
17	5.08	0.692	17	0.611
18	4.23	0.451	18	0.489
19	3.60	0.445	19	0.573
20	3.05	0.339	20	0.530
21	2.66	0.233	21	0.472
22	2.31	0.301	22	0.852
23	2.02	0.253	23	1.51
24	1.76	0.242	24	2.40
25	1.55	0.195	25	2.58
26	1.37	0.176	26	3.00
27	1.21	0.145	27	2.89
28	1.08	0.128	28	2.83
29	0.970	0.119	29	2.92
30	0.866	0.106	30	2.81
31	0.770	0.0727	31	2.07
32	0.690	0.0584	32	1.77
33	0.624	0.0486	33	1.57
34	0.564	0.0361	34	1.23
35	0.513	0.0315	35	1.14
36	0.469	0.0195	36	0.746
37	0.428	0.0241	37	0.969
38	0.394	0.0236	38	0.988
39	0.363	0.0218	39	0.947
40	0.335	0.0188	40	0.844
41	0.312	0.0207	41	0.942
42	0.289	0.0215	42	0.969
43	0.270	0.0192	43	0.820
44	0.251	0.0178	44	0.703
45	0.236	0.0182	45	0.658
46	0.219	0.0156	46	0.494
47	0.205	0.0149	47	0.430
48	0.192	0.0122	48	0.303
49	0.181	0.0135	49	0.280
50	0.170	0.0107	50	0.183
51	0.161	0.00980	51	0.127
52	0.152	0.00990	52	0.0938
53	0.144	0.0101	53	0.0508
54	0.138	0.0122	54	0.0188
55	0.130	0.0123	55	0.00810

TABLE B.V

PARTIAL KERMA IN ALUMINUM DUE TO THE AUGER EFFECT

$h\nu$ (kev)	$\frac{\tau_K}{\rho}$ (cm^2/g)	$\frac{\phi_K - \delta}{h\nu} = f^{Auger}\frac{\tau}{}$	$\frac{\tau_K}{\rho} f^{Auger}\frac{\tau}{}$ (cm^2/g)	$\bar{E}_o'$ (kev)	$\Delta K(\bar{E}_o')$ x 0.985 (ergs/g-R)
13	11.2	0.111	1.24	1.5	0.279
14	8.72	0.103	0.899	1.5	0.483
15	6.70	0.0960	0.644	1.5	0.393
16	5.60	0.0900	0.504	1.5	0.364
17	4.39	0.0846	0.372	1.5	0.328
18	3.78	0.0800	0.303	1.5	0.328
19	3.16	0.0757	0.239	1.5	0.308
20	2.71	0.0720	0.195	1.5	0.305
21	2.33	0.0686	0.160	1.5	0.324
22	2.01	0.0655	0.132	1.5	0.374
23	1.76	0.0626	0.110	1.5	0.657
24	1.53	0.0600	0.0918	1.5	0.912
25	1.35	0.0576	0.0776	1.5	1.03
26	1.19	0.0554	0.0659	1.5	1.12
27	1.06	0.0533	0.0565	1.5	1.12
28	0.945	0.0514	0.0485	1.5	1.07
29	0.844	0.0496	0.0418	1.5	1.02
30	0.753	0.0480	0.0362	1.5	0.961
31	0.690	0.0465	0.0321	1.5	0.915
32	0.624	0.0450	0.0281	1.5	0.853
33	0.567	0.0436	0.0247	1.5	0.797
34	0.518	0.0424	0.0220	1.5	0.750
35	0.472	0.0411	0.0194	1.5	0.702
36	0.430	0.0400	0.0172	1.5	0.658
37	0.394	0.0389	0.0153	1.5	0.615
38	0.360	0.0379	0.0136	1.5	0.569
39	0.331	0.0369	0.0122	1.5	0.530
40	0.305	0.0360	0.0110	1.5	0.494
41	0.281	0.0351	0.00990	1.5	0.451
42	0.259	0.0343	0.00890	1.5	0.401
43	0.239	0.0335	0.00800	1.5	0.342
44	0.221	0.0327	0.00720	1.5	0.285
45	0.206	0.0320	0.00660	1.5	0.239
46	0.191	0.0313	0.00600	1.5	0.190
47	0.178	0.0307	0.00550	1.5	0.159
48	0.167	0.0300	0.00500	1.5	0.124
49	0.155	0.0294	0.00460	1.5	0.0955
50	0.146	0.0288	0.00420	1.5	0.0719
51	0.137	0.0282	0.00390	1.5	0.0506
52	0.129	0.0277	0.00360	1.5	0.0341
53	0.120	0.0272	0.00330	1.5	0.0166
54	0.112	0.0267	0.00300	1.5	0.00460
55	0.104	0.0262	0.00270	1.5	0.00180

TABLE B.VI

PARTIAL KERMA IN ALUMINUM DUE TO THE COMPTON EFFECT

$h\nu$ (kev)	$\frac{\sigma}{\rho} f_c$ (cm^2/g)	$\bar{E}_o'$ (kev)	$\Delta K(\bar{E}_o')$ x 0.985 (ergs/g-R)
13	0.00440	0.31	0.00100
14	0.00470	0.36	0.00250
15	0.00510	0.40	0.00310
16	0.00530	0.46	0.00380
17	0.00560	0.52	0.00490
18	0.00590	0.58	0.00640
19	0.00620	0.64	0.00800
20	0.00650	0.70	0.0102
21	0.00680	0.78	0.0138
22	0.00710	0.85	0.0201
23	0.00730	0.94	0.0436
24	0.00750	1.02	0.0745
25	0.00780	1.11	0.104
26	0.00810	1.20	0.138
27	0.00830	1.30	0.165
28	0.00860	1.38	0.190
29	0.00880	1.50	0.215
30	0.00900	1.60	0.239
31	0.00920	1.68	0.262
32	0.00950	1.80	0.288
33	0.00970	1.90	0.313
34	0.00990	2.01	0.337
35	0.0101	2.12	0.366
36	0.0103	2.23	0.394
37	0.0106	2.35	0.426
38	0.0108	2.46	0.452
39	0.0110	2.58	0.478
40	0.0112	2.70	0.503
41	0.0114	2.82	0.519
42	0.0116	2.94	0.523
43	0.0118	3.06	0.504
44	0.0120	3.19	0.474
45	0.0122	3.32	0.441
46	0.0124	3.46	0.393
47	0.0126	3.58	0.364
48	0.0128	3.73	0.318
49	0.0129	3.86	0.268
50	0.0131	4.00	0.224
51	0.0133	4.15	0.173
52	0.0135	4.31	0.128
53	0.0136	4.47	0.0684
54	0.0138	4.62	0.0213
55	0.0140	4.78	0.00930

TABLE B.VII

PARTIAL KERMA IN IRON DUE TO THE K-SHELL PHOTOELECTRIC EFFECT

$h\nu$ (kev)	$\frac{\tau_K}{\rho}$ (cm^2/g)	$(1-\phi_K/h\nu) = f^K_\tau$	$\frac{\tau_K f^K_\tau}{\rho}$ (cm^2/g)	E_o' (kev)	$\Delta K(E_o')$ x 0.015 (ergs/g-R)
13	76.2	0.462	35.2	6	0.117
14	62.0	0.500	31.0	7	0.247
15	50.3	0.534	26.9	8	0.243
16	42.2	0.563	23.8	9	0.254
17	35.6	0.588	20.9	10	0.274
18	30.0	0.611	18.3	11	0.294
19	25.6	0.632	16.2	12	0.309
20	22.0	0.650	14.6	13	0.339
21	19.1	0.666	12.7	14	0.381
22	16.8	0.682	11.5	15	0.481
23	14.8	0.696	10.3	16	0.912
24	12.9	0.708	9.13	17	1.34
25	11.5	0.720	8.28	18	1.63
26	10.2	0.731	7.46	19	1.88
27	9.30	0.741	6.89	20	2.03
28	8.40	0.750	6.30	21	2.06
29	7.59	0.759	5.75	22	2.08
30	6.86	0.766	5.25	23	2.06
31	6.23	0.774	4.82	24	2.04
32	5.64	0.781	4.41	25	1.98
33	5.17	0.788	4.07	26	1.95
34	4.74	0.794	3.76	27	1.90
35	4.38	0.800	3.50	28	1.88
36	4.00	0.805	3.22	29	1.83
37	3.69	0.811	2.99	30	1.78
38	3.40	0.816	2.77	31	1.72
39	3.16	0.820	2.59	32	1.67
40	2.94	0.825	2.43	33	1.61
41	2.71	0.829	2.25	34	1.52
42	2.52	0.833	2.10	35	1.40
43	2.36	0.837	1.98	36	1.25
44	2.20	0.841	1.85	37	1.08
45	2.05	0.844	1.73	38	0.927
46	1.91	0.848	1.62	39	0.760
47	1.79	0.851	1.52	40	0.651
48	1.69	0.854	1.44	41	0.531
49	1.58	0.857	1.35	42	0.417
50	1.48	0.860	1.27	43	0.323
51	1.39	0.863	1.20	44	0.231
52	1.31	0.865	1.13	45	0.159
53	1.22	0.868	1.06	46	0.0789
54	1.17	0.870	1.02	47	0.0233
55	1.10	0.873	0.960	48	0.00940

TABLE B.VIII

PARTIAL KERMA IN IRON DUE TO THE L-SHELL PHOTOELECTRIC EFFECT

$h\nu$ (kev)	$\frac{\mu_K}{\rho}$ (cm^2/g)	$\frac{\tau_L}{\rho}$ (cm^2/g)	$f_\tau^L = (1-\phi_L/h\nu)$	$\frac{\tau_L}{\rho} f_\tau^L$ (cm^2/g)	E_o' (kev)	$\Delta K(E_o')$ x 0.015 (ergs/g-R)
13	75.0	28.1	0.938	26.4	12.2	0.0880
14	62.2	22.4	0.943	21.1	13.2	0.168
15	50.9	17.3	0.947	16.4	14.2	0.148
16	43.2	14.2	0.950	13.5	15.2	0.144
17	36.6	11.5	0.953	10.9	16.2	0.143
18	31.2	9.53	0.956	9.11	17.2	0.146
19	26.7	7.83	0.958	7.50	18.2	0.143
20	22.6	5.77	0.960	5.54	19.2	0.129
21	20.0	5.46	0.962	5.26	20.2	0.158
22	17.6	4.61	0.964	4.45	21.2	0.187
23	15.3	3.71	0.965	3.58	22.2	0.317
24	13.7	3.49	0.967	3.38	23.2	0.498
25	12.1	2.90	0.968	2.81	24.2	0.551
26	10.9	2.65	0.969	2.57	25.2	0.649
27	9.75	2.17	0.970	2.10	26.2	0.619
28	8.79	1.88	0.971	1.83	27.2	0.600
29	7.98	1.70	0.972	1.65	28.2	0.599
30	7.30	1.59	0.973	1.54	29.2	0.607
31	6.63	1.40	0.974	1.36	30.2	0.577
32	6.10	1.33	0.975	1.30	31.2	0.585
33	5.59	1.19	0.976	1.17	32.2	0.558
34	5.14	1.09	0.976	1.06	33.2	0.537
35	4.75	0.987	0.977	0.965	34.2	0.517
36	4.39	0.939	0.978	0.918	35.2	0.521
37	4.01	0.808	0.978	0.791	36.2	0.471
38	3.71	0.747	0.979	0.732	37.2	0.453
39	3.42	0.657	0.979	0.643	38.2	0.414
40	3.16	0.577	0.980	0.566	39.2	0.376
41	2.93	0.540	0.980	0.530	40.2	0.357
42	2.71	0.480	0.981	0.471	41.2	0.315
43	2.52	0.424	0.981	0.416	42.2	0.264
44	2.36	0.399	0.982	0.392	43.2	0.229
45	2.20	0.368	0.982	0.361	44.2	0.194
46	2.05	0.335	0.983	0.330	45.2	0.155
47	1.92	0.309	0.983	0.304	46.2	0.130
48	1.80	0.275	0.983	0.270	47.2	0.0994
49	1.69	0.259	0.984	0.255	48.2	0.0785
50	1.59	0.245	0.984	0.242	49.2	0.0613
51	1.50	0.233	0.984	0.229	50.2	0.0441
52	1.41	0.214	0.985	0.211	51.2	0.0296
53	1.33	0.212	0.985	0.209	52.2	0.0155
54	1.26	0.186	0.985	0.183	53.2	0.00420
55	1.20	0.186	0.985	0.184	54.2	0.00180

TABLE B.IX

PARTIAL KERMA IN IRON DUE TO THE AUGER EFFECT

$h\nu$ (kev)	$\frac{\tau_K}{\rho}$ (cm^2/g)	$\frac{\phi_K - \delta}{h\nu} = f_{\tau}^{Auger}$	$\frac{\tau_K f_{\tau}^{Auger}}{\rho}$ (cm^2/g)	$\bar{E}_o'$ (kev)	$\Delta K(\bar{E}_o')$ x 0.015 (ergs/g-R)
13	76.2	0.153	11.6	6.5	0.0389
14	62.0	0.142	8.80	6.5	0.0701
15	50.3	0.133	6.69	6.5	0.0604
16	42.2	0.124	5.23	6.5	0.0560
17	35.6	0.117	4.17	6.5	0.0545
18	30.0	0.111	3.33	6.5	0.0535
19	25.6	0.105	2.69	6.5	0.0513
20	22.0	0.0995	2.19	6.5	0.0508
21	19.1	0.0948	1.81	6.5	0.0543
22	16.8	0.0904	1.52	6.5	0.0637
23	14.8	0.0865	1.28	6.5	0.113
24	12.9	0.0828	1.07	6.5	0.157
25	11.5	0.0795	0.914	6.5	0.180
26	10.2	0.0765	0.780	6.5	0.197
27	9.30	0.0737	0.685	6.5	0.202
28	8.40	0.0710	0.596	6.5	0.196
29	7.59	0.0686	0.521	6.5	0.189
30	6.86	0.0663	0.455	6.5	0.179
31	6.23	0.0642	0.400	6.5	0.169
32	5.64	0.0622	0.351	6.5	0.158
33	5.17	0.0603	0.312	6.5	0.149
34	4.74	0.0585	0.277	6.5	0.140
35	4.38	0.0568	0.249	6.5	0.133
36	4.00	0.0553	0.221	6.5	0.125
37	3.69	0.0538	0.199	6.5	0.118
38	3.40	0.0524	0.178	6.5	0.111
39	3.16	0.0510	0.161	6.5	0.104
40	2.94	0.0497	0.146	6.5	0.0972
41	2.71	0.0486	0.132	6.5	0.0888
42	2.52	0.0474	0.119	6.5	0.0797
43	2.36	0.0463	0.109	6.5	0.0692
44	2.20	0.0452	0.0994	6.5	0.0582
45	2.05	0.0442	0.0906	6.5	0.0486
46	1.91	0.0433	0.0827	6.5	0.0388
47	1.79	0.0423	0.0757	6.5	0.0324
48	1.69	0.0415	0.0701	6.5	0.0258
49	1.58	0.0406	0.0641	6.5	0.0197
50	1.48	0.0398	0.0589	6.5	0.0149
51	1.39	0.0390	0.0542	6.5	0.0104
52	1.31	0.0383	0.0502	6.5	0.00700
53	1.22	0.0376	0.0459	6.5	0.00340
54	1.17	0.0369	0.0432	6.5	0.00100
55	1.10	0.0362	0.0398	6.5	0.000400

TABLE B.X

PARTIAL KERMA IN IRON DUE TO THE COMPTON EFFECT

$h\nu$ (kev)	$\frac{\sigma}{\rho} f_c$ (cm^2/g)	$\bar{E}_o'$ (kev)	$\Delta K(\bar{E}_o')$ x 0.015 (ergs/g-R)
13	0.00430	0.31	0.0000
14	0.00460	0.36	0.0000
15	0.00490	0.40	0.0000
16	0.00510	0.46	0.0001
17	0.00540	0.52	0.0001
18	0.00570	0.58	0.0001
19	0.00600	0.64	0.0001
20	0.00630	0.70	0.0001
21	0.00650	0.78	0.0002
22	0.00680	0.85	0.0003
23	0.00710	0.94	0.0006
24	0.00730	1.02	0.0011
25	0.00750	1.11	0.0015
26	0.00780	1.20	0.0020
27	0.00800	1.30	0.0024
28	0.00830	1.38	0.0027
29	0.00850	1.50	0.0031
30	0.00870	1.60	0.0034
31	0.00890	1.68	0.0038
32	0.00910	1.80	0.0041
33	0.00940	1.90	0.0045
34	0.00960	2.01	0.0048
35	0.00980	2.12	0.0053
36	0.0100	2.23	0.0057
37	0.0102	2.35	0.0061
38	0.0104	2.46	0.0064
39	0.0106	2.58	0.0068
40	0.0108	2.70	0.0072
41	0.0110	2.82	0.0074
42	0.0112	2.94	0.0075
43	0.0114	3.06	0.0072
44	0.0116	3.19	0.0068
45	0.0118	3.32	0.0063
46	0.0119	3.46	0.0056
47	0.0121	3.58	0.0052
48	0.0123	3.73	0.0045
49	0.0125	3.86	0.0038
50	0.0127	4.00	0.0032
51	0.0128	4.15	0.0025
52	0.0130	4.31	0.0018
53	0.0132	4.47	0.0010
54	0.0133	4.62	0.0003
55	0.0135	4.78	0.0001

BIBLIOGRAPHY

Berger, R.T., 1961, Rad. Res., 15, 1.

Berger, M.J., and Seltzer, S.M., 1964, National Aeronautics and Space Administration, Washington, D.C., Report SP-3012.

Bragg, W., 1912, Studies in Radioactivity (London, Macmillan), pp. 94 ff.

Burlin, T.E., 1966, Phys. Med. Biol., 11, 2, 255.

Charlton, D.E., and Cormack, D.V., 1962, Rad. Res., 17, 34.

Charlton, D.E., 1967, (Ph.D. thesis, University of Saskatchewan).

Evans, R.D., 1958, in Handbuch der Physik, (S. Flugge, ed.), (Burlin, Springer-Verlag), 34, 218.

Epp, E.R., and Weiss, H.W., 1966, Phys. Med. Biol., 2, 225.

Freedman, M.S., Novey, T.B., Porter, F.T., and Wagner, F., 1956, The Review of Scientific Instruments, 27, 9, 716.

Gray, L.H., 1929, Proc. Roy. Soc., A122, 647.

Grodstein, G.W., 1957, National Bureau of Standards (U.S.), Circular 583.

Howarth, J.L., 1965, Rad. Res., 24, 158.

International Commission on Radiological Units and Measurements, 1962, National Bureau of Standards (U.S.), Report 10a, Handbook 84.

Shafroth, S.M., 1967, Scintillation Spectroscopy of Gamma Radiation, (London, New York, Gordon and Breach Science Publishers), pp. 289-291.

Skarsgard, L.D., Johns, H.E., and Green, L.E.S., 1961, Rad. Res., 14, 261.

Spencer, L.V., and Attix, F.H., 1955, Rad. Res., 3, 239.